Diplomarbeit

„Measurements of Extinction of Premixed Flames Burning High Molecular Weight Hydrocarbon Fuels"

ausgeführt zum Zwecke der Erlangung des akademischen Grades eines Diplom-Ingenieurs unter der Leitung von

ao. Univ.-Prof. Dipl.-Ing. Dr. techn. Ernst Pucher
Institut für Verbrennungskraftmaschinen und Kraftfahrzeugbau der Technischen Universität Wien

und

Prof. Dr. Kalyanasundaram Seshadri
Department of Mechanical and Aerospace Engineering,
Center for Energy Research
University of California, San Diego

eingereicht an der Technischen Universität Wien

Fakultät für Maschinenbau

von

Patrick Weydert
Matrikelnummer: 0526991
31, Rue du Bois
L-6943 Niederanven

Wien, am 14. Oktober 2008

Measurements of Extinction of Premixed Flames Burning High Molecular Weight Hydrocarbon Fuels

Diploma Thesis

Institute for Internal Combustion Engines and
Automotive Engineering

Vienna University of Technology, Austria

Patrick Weydert

Prof. Dr. Ernst Pucher
Institute for Internal Combustion Engines and Automotive
Engineering
Vienna University of Technology, Austria

Prof. Dr. Kalyanasundaram Seshadri
Department of Mechanical and Aerospace Engineering,
Center for Energy Research
University of California, San Diego

Vienna, October 2008

Abstract

Extinction points of premixed flames for different hydrocarbon fuels were analyzed in this study.

The experiments were done using a setup where a pure nitrogen flow streams against a fuel/oxygen/nitrogen mixture flow. A premixed flame is stabilized between two ducts of the counter flow setup. The calculation was done on a computer program called Chemkin 4.1.1 with which these kind of experiments can be simulated. Critical conditions of extinction were measured and calculated.

Nine different fuels were experimentally tested, the multi component fuel JP-8, fuel mixtures (surrogates) Surrogate C and Aachen Surrogate and the pure fuels n-Heptane, n-Decane, n-Dodecane, Methylcyclohexane, o-Xylene, and 1,2,4-Trimethylbenzene which are the components of the two surrogates except for n-Heptane.

The experiments were done for different fuel-air ratios while the flow velocity of the gases is increased until extinction is observed.

Numerical calculation was done for n-Heptane on Chemkin 4.1.1 and for n-Decane by Alessio Frassoldati and coworkers (Politecnico di Milano, Dipartimento di Chimica).
Numerical and experimental results were compared. For n-Heptane the numerical data over predicts the experimental data up to a fuel-air ratio Φ of 1.1. In the region above, both data agree very well. The numerical and experimental data for o-Xylene agree very well with each other for all Φ. For n-Decane the numerical data over predicts the experimental data in a region of Φ > 1.1. Between Φ = 0.9 to 1.1 both data agree very well.

Zusammenfassung

In dieser Studie wurden verschiedene Kraftstoffe mit Vormischflamme auf Flammabriss getestet. Die Versuche wurden nach dem Gegenstromprinzip durchgeführt wobei purer Stickstoff auf eine Kraftstoffmischung, bestehend aus Kraftstoff, Sauerstoff und Stickstoff trifft. Dadurch entsteht zwischen beiden Auslässen eine Stagnationsebene unter der eine Flamme stabilisiert werden kann. Die Versuche wurden für verschiedene Luftverhältnisse ermittelt wobei jedes Mal die Flussgeschwindigkeit bis zum Flammabriss erhöht wurde. Die numerische Berechnung für n-Heptan wurde mit Hilfe vom Computerprogramm Chemkin 4.1.1 durchgeführt, während die Berechnungen für o-Xylen und n-Dekan von Alessio Frassoldati und Mitarbeiter (Politecnico di Milano, Dipartimento di Chimica) durchgeführt wurden.

Insgesamt wurden neun verschiedene Kraftstoffe gemessen, Mehrkomponentenkraftstoff (Jetkraftstoff) JP-8, die aus zwei beziehungsweise drei Kohlenwasserstoffen bestehende Ersatzkraftstoffe für JP-8: „Aachen Surrogate" und „Surrogate C" sowie die reinen Kraftstoffe: n-Dekan, n-Dodekan, n-Heptan, Methylcyclohexan, o-Xylen und 1,2,4-Trimethylbenzen. Dabei sind die reinen Kraftstoffe die Bestandteile der Ersatzkraftstoffe mit Ausnahme von n-Heptan.

Die Ergebnisse aus Berechnung und Experiment wurden miteinander verglichen. Beim Vergleich der Werte für n-Heptan stellte sich heraus, dass bis zu einem Luftverhältnis von Φ = 1.1 der Flammabriss im Versuch viel eher eintritt als bei der Berechnung. Bei $\Phi > 1.1$ stimmen beide Ergebnisse gut überein. Bei den Berechnungen für o-Xylen und n-Dekan von Alessio Frassoldati und Mitarbeiter stimmen Berechnung und Versuch für o-Xylen im gesamten Luftverhältnisbereich sehr gut überein während für n-Dekan der Flammabriss im Luftverhältnisbereich $\Phi > 1.1$ etwas eher beim Versuch eintritt als bei der Berechnung.

Acknowledgements

Contents:

List of Symbols

T	temperature
a	strain rate
N	Nitrogen
O	Oxygen
H	Hydrogen
C	Carbon
L	separation distance
p	pressure
Φ	equivalence ratio
Y	mass fraction
x	radial coordinate
MW	molar weight
ρ	density
V	radial velocity
RH	large aliphatic hydrocarbon
RCH_3	aromatic hydrocarbon
$R\cdot$	radical
$R'\cdot$	small radical
Y_{ox}	dilution of air and nitrogen
$d_{exhaust}$	diameter of the exhaust duct
$d_{curtain}$	diameter of the curtain duct
d_{fuel}	diameter of the fuel duct
ETC.	et cetera
M	chemical species

Subscripts

1	fuel mixture side
2	inert side
max	maximum
fuel	fuel
n-Decane	n-Decane
O_2	Oxygen
N_2	Nitrogen
n	number of atoms

1. Introduction

The United States Department of Defense (DOD) decided in their directive #4140.25 that only one primary fuel should be used to power all land-based air and ground forces vehicles. The fuel should be a kerosene-based fuel, either JP-8, commercial jet fuel with additives or commercial jet fuel without additives. JP-8 and Commercial Jet Fuels were already tested for non-premixed flames. The conclusion of this study was that those fuels have similar critical conditions of extinction and auto ignition in non-premixed flames. [1]

The task is therefore to develop technologies so that the U.S. Army can use JP-8 in all their ground vehicles and unmanned aerial vehicles (UAV). Currently the UAV's are powered with gasoline or specialty fuels. It is very likely that UAV's will employ internal combustion engines that use spark-ignition or compression-ignition. Many fuel properties like combustion, fuel injection, or lubricity have to be considered to get an optimal result. In the present study extinction of premixed flames are tested.

Therefore, it is of high importance to develop so called surrogate fuels which are mixtures of only a few hydrocarbons. Fuel surrogate types may be defined as follows [2]:

1. Physical surrogate which have the same physical properties (such as density) as the desired commercial fuels. [2]
2. Chemical surrogate which have the same chemical properties (such as combustion) as the desired commercial fuels. [2]

Surrogates with only two components have been found to reproduce many aspects of combustion of jet fuels very well. [1, 3, 4]

JP-8, Jet Fuel and 15 different surrogates have been tested in non-premixed flames. A non-premixed flame is a flame where oxygen is mixed with fuel by convection and diffusion. That's why non-premixed flames are also called diffusion flames. An example for a diffusion flame is a candle. [1, 5]

For two of these 15 surrogates extinction-, auto ignition behavior agreed well with JP-8. Furthermore, a comparison on the hydrogen to carbon ratio H/C (table 1) is done, to select surrogates which fit best with JP-8. These surrogates are: Surrogate C which is made up of 60% n-Dodecane, 20% Methylcyclohexane, and 20% o-Xylene by volume with a H/C ratio of 1.92 and Aachen Surrogate which is made up of 80% n-Decane and 20% 1,2,4-Trimethylbenzene by weight with a H/C ratio 1.99. [1]

Fuel	JP-8	Aachen Surrogate	Surrogate C
H/C ratio	1.91	1.99	1.92

**Table 1** *Hydrogen to carbon ratios H/C for JP-8, Aachen Surrogate and surrogate C*

Two surrogates and their components as well as JP-8 and n-Heptane are tested for premixed flames in the present study.

2. Hydrocarbon Fuels

2.1 Combustion of Hydrocarbons

The combustion of hydrocarbon fuels requires a defined temperature for every reaction. The reaction rates for the oxidation increase with higher temperatures. Combustion reactions of aliphatic hydrocarbons only vary a little from each other whereas a significant difference between the combustion of aliphatic and aromatic hydrocarbons can be noted. [6]

The combustion of larger aliphatic hydrocarbons RH, like tested in this study, starts with attacking the C-H bonds by H, O, OH, HO_2 atoms at high temperatures to form radicals R·

$$RH + (H, O, OH, HO_2) \rightarrow R· + (H_2, OH, H_2O, H_2O_2).$$
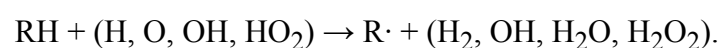
Those are then thermally decomposed (into at least two substances) to an alkene and smaller R'· (via β decomposition) until smaller hydrocarbons (alkyls(radicals): $C_nH_{2n}+1$) like methyl and ethyl are reached. These are then oxidized as well. For chain straight aliphatic fuels, the C-C bonds most likely break first due to their lower bond energy compared to C-H bonds. Due to the fact that larger hydrocarbon molecules and radicals quickly decompose to smaller molecules and radicals the combustion behavior of larger hydrocarbons varies little with the fuel. The reason of this is that larger hydrocarbons more likely break into smaller more reactive pieces than smaller hydrocarbons. Figure 1 shows the decomposition of alkanes to the relative stable methyl and ethyl. [7, 8, 9]
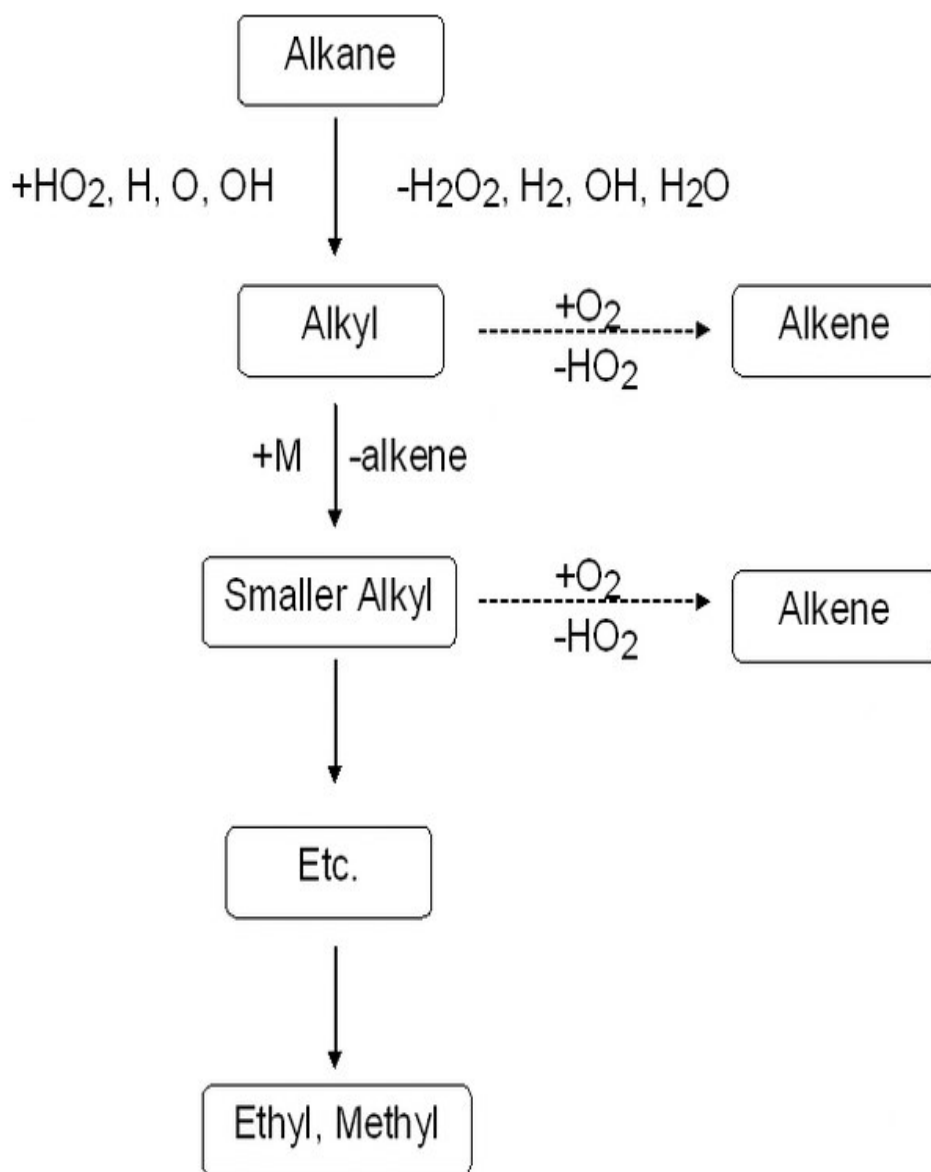
Figure 1 *Schematic mechanism of the radical pyrolysis of a large aliphatic hydrocarbon to form ehtyl and methyl.* [7]

Much less is known about the oxidation of aromatic hydrocarbons [7]. Aromatics have a higher carbon to hydrogen number than aliphatics, which means that flames of aromatic fuels are sootier than their corresponding aliphatic flames. The side chains of aromatic compounds get oxidized first in the same way like aliphatics

$$RCH_3 + (O, OH) \rightarrow RCH_2 + (H_2, H_2O).$$
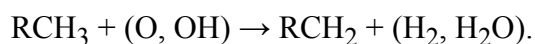
When all the side chains are oxidized, the aromatic ring also gets oxidized. Aromatics are less reactive than their aliphatics analogues compounds due to the chemical resonance phenomena. [8, 9]

The numerical simulation of premixed flames is done with special computer programs like Chemkin. Complex numerical mechanisms to simulate chemical reactions are used in these computer programs. The larger the hydrocarbon chain, the more reactions, hence the more complex is the mechanism. For writing such chemical mechanisms, information about their reactions must be known. Each fuel has its own mechanism; however, most mechanisms are based on others. For example mechanisms for smaller alkanes are the building stone for higher alkanes. The mechanisms contain different chemical reactions which describe the combustion of the appropriate fuel.

2.2 Fuels

2.2.1 Hydrocarbons

Hydrocarbons are compounds which only contain carbon and hydrogen atoms. Hydrocarbons can be classified in saturated and unsaturated hydrocarbons. [10]

Saturated Hydrocarbons (or aliphatic compounds)

In the organic chemistry saturated means that the hydrocarbon has the maximum number of hydrogen molecules for the number of carbon molecules it consists of. Saturated hydrocarbons consist of only single bonds and can again be classified in alkanes and cyclalkanes:

Alkanes (or paraffins)

The carbon atoms build a straight chain. The general formula for alkanes is C_nH_{2n+2}. Compounds with the same molecular formula and more than four carbons can have different structural formulas. These compounds are called isomers and have branched chains. [10, 11]

Cycloalkanes (or naphtenes)

A cycloalkane is a saturated hydrocarbon where the carbon atoms build a ring instead of a straight chain. The general formula of a cycloalkane is C_nH_{2n}. Their names are given by adding the term "cyclo" to the name of the appending alkane. Cyclohexanes are represented by a hexagon due to the number of carbons. [10, 11]

Unstaturated Hydrocarbons

Unsaturated hydrocarbons contsists of one or more C-C double or triple bonds. Unsaturated means that there are fewer hydrogen molecules attached to the carbon skeleton than in an alkane. There are 3 classes of unsaturated hydrocarbons: alkenes, alkynes and arenes (or aromatics). Benzene belongs to the class of the arenes (aromatics). Benzene consists of a ring structure with the formula C_6H_6. Benzene is the basis for several compounds where one or more hydrogen atoms are replaced by a molecule or an atom. [10, 11]

Aliphatics in this study

Aliphatics in this study are: n-Heptane, n-Decane, n-Dodecane and the cycloalkane; Methylcyclohexane. The properties of the different saturated hydrocarbons and their chemical structure can be seen in Table 2 and Figure 2. (Data in this table from [12])

Compound	Formula	MW [g/mol]	Boiling point [K]	Density at 25°C [g/ml]
Alkanes**:**				
n-Heptane	C_7H_{16}	100.204	371.58	0.682
n-Decane	$C_{10}H_{22}$	142.285	447.30	0.728
n-Dodecane	$C_{12}H_{26}$	170.338	489.47	0.745
Cycloalkane:				
Methylcyclohexane	C_7H_{14}	98.188	374.08	0.766

Table 2 *Properties of the aliphatic compounds*

N-Heptane, n-Decane and n-Dodecane are alkanes with one unbranched carbon chain. N-Heptane has 7 carbon atoms and 16 hydrogen atoms, n-Decane has 10 carbon atoms and 22 hydrogen atoms and n-Dodecane has 12 carbon atoms and 26 hydrogen atoms. That means, that n-Heptane has the shortest chain of this three compounds, n-Decane the second longest and n-Dodecane has the longest chain. Therefore, n-Heptane has the lowest molecular weight, n-Decane the second highest and n-Dodecane the highest molecular weight when comparing these three compounds.

Methylcyclohexane has a ring structure with 7 carbon atoms and 14 hydrogen atoms. The ring is a hexagon with one additional methyl group.
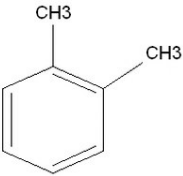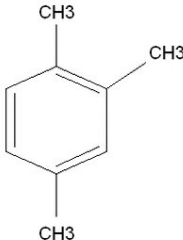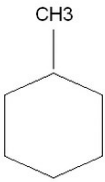
Aromatics in this study

Properties, chemical structures, and formulas of the aromatic compounds are noted in Table 3 and Figure 2.

Compound	Formula	MW [g/mol]	Boiling point [K]	Density at 25°C [g/ml]
Aromatics:				
o-Xylene	C_8H_{10}	106.167	417.58	0.876
1,2,4-Trimethylbenzene	C_9H_{12}	120.194	442.53	0.872

Table 3 *Properties of the aromatics.* (Data in this table from [12])

1, 2, 4-Trimethylbenzene has 9 carbon atoms and 12 hydrogen atoms. It is based on a benzene ring with 3 methyl groups attached at the first, second and fourth carbons in the ring. O-Xylene or ortho-Xylene has 8 carbon atoms and 10 hydrogen atoms and is also based on a benzene ring but with only two methyl groups attached on the first and second carbon in the ring.

Aliphatics	Aromatics
n-Heptane: C_7H_{16}	o-Xylene: C_8H_{10}
n-Decane: $C_{10}H_{22}$	1,2,4-Trimethlbenzene: C_9H_{12}
n-Dodecane: $C_{12}H_{26}$	
Methylcyclohexane: C_7H_{14}	

Figure 2 *Chemical structures and formulas of the compounds*

2.2.2 Jet fuels

Military and commercial jet fuels are almost exclusively produced from kerosene fraction of crude oil (table 4). Key requirements focus on sulfur and aromatics contents, clean burning characteristics and storage stability. Refineries use increasingly hydro treating technology as well as crude state selection to meet specifications and aircraft powered demand. Legislative reduction in sulfur and aromatics is not currently anticipated. [13]

Jet Fuel	
Property	**Value**
Density	775-840 [kg/m^3]
Final Boiling Point	288-300 [°C] max
Flash Point	38-60 [°C] min
Aromatics	20-25 [%] by volume, max
Sulfur	0.3-0.4 [%] by weight, max
Mercaptan Sulfur	0.002 [%] by weight max
Freeze Point	-40 to -47 [°C] max

Table 4 *Jet fuel specifications.* [13]

Crude oil

Crude oil is composed of aromatic, alkanes and cycloalkanes hydrocarbons. Minor amounts of olefins may be present. Average aromatics content is about 50 %, however, it can range from as low as 25 % to as much as 75 %. High gravity crude (thin crude) oils are easier to refine because they contain more of the lighter products and have lower sulfur and nitrogen content. However, low gravity crude (thick crude) oils can nowadays also be refined into high-value products. But this requires more complex and expensive processing equipment, more processing steps and energy what makes it more expensive. The alkane cycloalkane ratio is widely ranging and is qualitatively identified via the labeling of many crudes as "alkanic" or "cycloalkanic". Hydrocarbon composition affects many considerations in selecting processing options, or meeting product specifications. [13, 14]

Processing

Jet Fuel processing starts with separation of crude oil by distillation, with the jet fuel fraction in the 150-290 [K] boiling range. Depending on the crude, a few such streams are directly suitable as jet fuel, but most require further treating. Sulfur-containing compounds are very corrosive and are therefore converted to the less corrosive disulfides by several different processes like hydro cracking or Merox (mercaptan oxidation). All these processes work as catalyst processes and remove sulfur from the original compounds. For Merox by using a cobalt-based and hydro cracking uses a catalyst and hydrogen. An increasing number of refineries are hydro cracking hydrocarbons with higher boiling points to make high quality jet fuel with good low temperature characteristics. Unless a refinery makes jet fuel by hydro cracking, jet fuel yield and quality are dependent on product boiling range and on the crude slate. Availability is maximized by making a product with the widest possible boiling range. In turn, the boiling point tends to be limited on the low distillation end by the flash point, while the maximum distillation end point is controlled by the specific freezing point. Many refineries make a single product saleable as jet fuel, commercial kerosene, or diesel blending stock by having this product meet the specifications for the other products. Such a product is referred to as dual branded kerosene and is divided and supplied to the differing uses at the distribution terminal. [13, 14]

2.2.3 JP-8 and Surrogates

JP-8 (Jet Propulsion-8)

The development of the turbine engine for aircraft began independently in Germany and Britain in the 1930s. Illuminating kerosene, produced for wicked lamps, was used to fuel the first turbine engines. Since the engines were thought to be relatively insensitive to fuel properties, kerosene was chosen mainly because of availability; the war effort required every drop of gasoline. After World War II, the U.S. Air Force started using "wide-cut" fuel, which is essentially a hydrocarbon mixture spanning the gasoline and kerosene boiling ranges. The choice was driven by consideration of availability. Compared to a kerosene type fuel, wide-cut jet fuel had operational disadvantages. So the Air Force started to change back to kerosene-type fuel in the 1970s and has essentially completed the process of converting from wide-cut (JP-4) to kerosene (JP-8) system-wide. [14]

Today, the Air Force operates almost entirely on JP-8; in fact, this grade has become the primary battlefield fuel to be used in gas turbine and diesel powered ground vehicles as well as combat aircraft. The progression of U.S. Military fuels is illustrated in Table 5. Both, JP-3 and JP-4, which are blends of kerosene and naphton, reflected Air Force concern over fuel availability, while JP-5 is tailored to Navy requirements for carrier combat safety. JP-7 is a supersonic fuel in very limited use. [13]

Date of issue	Grade	Specification	Nato Symbol	Volatility and Freeze Point
1944	JP-1*	AN-F-32, changed to MIL-F-5616	-	110°F min flash -60°C max freeze
1946	JP-2*	Not issued	-	2 psi max RVP
1947	JP-3*	AN-F-58, changed to MIL-F-5624	-	5-7 psi RVP
1951	JP-4	MIL-F-5624, now MIL-PRF-5624	F-40	2-3 psi RVP
1952	JP-5	MIL-F-	F-44	140°F min flash -46°C max freeze
1956	JP-6*	MIL-F-2565	-	High thermal sta. -54°C max freeze
1980	JP-7	MIL-T-38219, now MIL-PRF-38219	-	140°F min flash -43°C max freeze
1979	JP-8	MIL-T-83133, now MIL-DTL-83133	F-34	100°F min flash -47°C max freeze

canceled. [13]

Table 5 *U.S. Military Jet Fuels* [13]

Kerosine fuels like JP-8 are mixtures of thousands of hydrocarbons. For JP-8, these hydrocarbons can be divided into three classes: aromatics (about 20 %), n-alkanes and isoalkanes (60 %), and cycloalkanes (napthenes, 20 %). The major difference between military fuels and commercial fuels consists in the use of additives. Otherwise, JP-8 and Jet A-1 are very similar (Table 6). [14, 15]

The JP-8 tested in this study was obtained from Wright Patterson Air Force Base (WPAFB) and is named JP-8 POSF 4177.

Additive Type	Jet A	Jet A-1	JP-4	JP-5	JP-8
Antioxidant	Allowed	Required*	Required*	Required*	Required*
Metal deactivator	Allowed	Allowed	Agreement	Agreement	Agreement
Electrical conductivity/ static dissipator	Allowed	Required	Required	Agreement	Required
Corrosion inhibtor/ lubrictiy improver	Agreement	Allowed	Required	Required	Required
Fuel system icing inhibitor	Agreement	Agreement	Required	Required	Required
Biocide	Agreement	Agreement	Not allowed	Not allowed	Not allowed
Thermal stability	Not allowed	Not allowed	Not allowed	Not allowed	Agreement**

* Required in any fuel, or fuel component, that has been hydroprocessed, otherwise optional

** When thermal stability additive is in JP-8, the fuel is called JP-8+100

Table 6 *Additive Types for Jet Fuels.* [14]

Surrogates

Table 7 shows the components of the Aachen Surrogate and Surrogate C.

	n-Decane	**n-Dodecane**	**Methylcyclo-hexane**	**o-Xylene**	**1,2,4-Trimethylbenzene**
Surrogate C	-	60 %	20 %	20 %	-
Aachen Surrogate	80 %	-	-	-	20 %

Table 7 *Composition of the Surrogates*

Surrogate C

Surrogate C is a mixture of 60 % n-Dodecane, 20 % Methylcyclohexane and 20 % of o-Xylene made up by volume. It consists of two saturated hydrocarbons, n-Dodecane and Methylcyclohexane and of one unsaturated hydrocarbon, o-Xylene. The H/C ratio is 1.92

Aachen surrogate

Aachen Surrogate is a mixture of 80 % n-Decane and 20 % of 1,2,4-Trimethylbenzene made up by weight. Aachen surrogate only consists of two compounds, one saturated hydrocarbon, n-Decane and one unsaturated hydrocarbon, 1,2,4-Trimethylbenzene. The H/C ratio for the Aachen Surrogate is 1.99.

2.3 FAR (fuel- air ratio)

A mixture of fuel in air can be expressed by the fuel-air ratio (FAR). The equivalence ratio is defined as the ratio of the fuel-to-oxidizer ratio to the stoichiometric fuel-to-air ratio:

$$\Phi = \frac{fuel-to-oxidizer-ratio}{\left(fuel-to-oxidizer-ratio\right)_{stoichiometric}}$$

$$\Phi = \frac{Y_{fuel}/Y_{oxidizer}}{\left(Y_{fuel}/Y_{oxidizer}\right)_{stoichiometric}}$$

$\Phi > 1$ represents an excess of fuel in the fuel-oxygen mixture and $\Phi < 1$ means a deficiency of fuel (excess of oxygen).

2.4 Premixed Flame

Even though flames in one form or another have been known and used since antiquity, a particularly simple form of combustion, the premixed gas flame, has been recognized and studied for only about 150 years. Its discovery was a side result of the researches of Berthollet, Dalton, Volta, and others (1776-1810) concerning the composition of combustible gases from different sources, particularly marsh gas (methane) and olefiant gas (ethylene). In their analyses, a combustible mixture of these gases with air was sparked in a bulb and the products of the premixed flame (explosion) were analyzed to determine the composition of the original combustible gas. During a later period (1805-1819) Davy's observation that a premixed flame would not propagate through a fine-mesh screen led to the invention of the safety lamp for mines. The "discovery" of the premixed flames was essentially completed in 1855 by Bunsen's invention of a burner which allowed the stabilization of a premixed flame in a flow system. [16]

Premixed-gas flames occur in mixtures of fuel, oxidant, and inert gases that are intimately mixed on the molecular scale before combustion is initiated. Examples of premixed-gas flames include Bunsen flames, gas appliance stoves, and gasoline fueled internal combustion engines. Accidental explosions that occur in mine shafts and chemical refineries are also premixed-gas flames that undergo a transition to a detonation. [17]

In the present study nine different fuels were tested. Oxygen was used as oxidant and nitrogen as the inert gas. This fuel/oxygen/nitrogen mixture is characterized by the equivalence ratio Φ and the dilution of oxygen with nitrogen which is given by the mass fractions Y_{O2} and Y_{N2}:

$$Y_{ox} = \frac{Y_{O_2}}{Y_{O_2} + Y_{N_2}}$$

The premixed flame can be divided into 2 zones, the preheat zone and the reaction zone. [9, 18]

1. Preheat zone is the zone where the mixture is heated up through convection of the reaction zone. No reactions take place in this zone due to the low temperature.

2. Reaction zone is a very narrow zone in which the chemical reactions take place. Thus the oxidations take place. This is also the zone in which the flame occurs (luminous zone) and where the highest temperature is reached. The color of the luminous zone changes with the fuel-oxidizer ratio. A fuel lean mixture has a deep blue or violet color due to the excited CH radicals and a fuel rich flame has a light blue or green color due to the C_2 molecule.

Figure 3 shows a graph of the 2 zones of a premixed flame. The maximal flame temperature is plotted over the distance x.
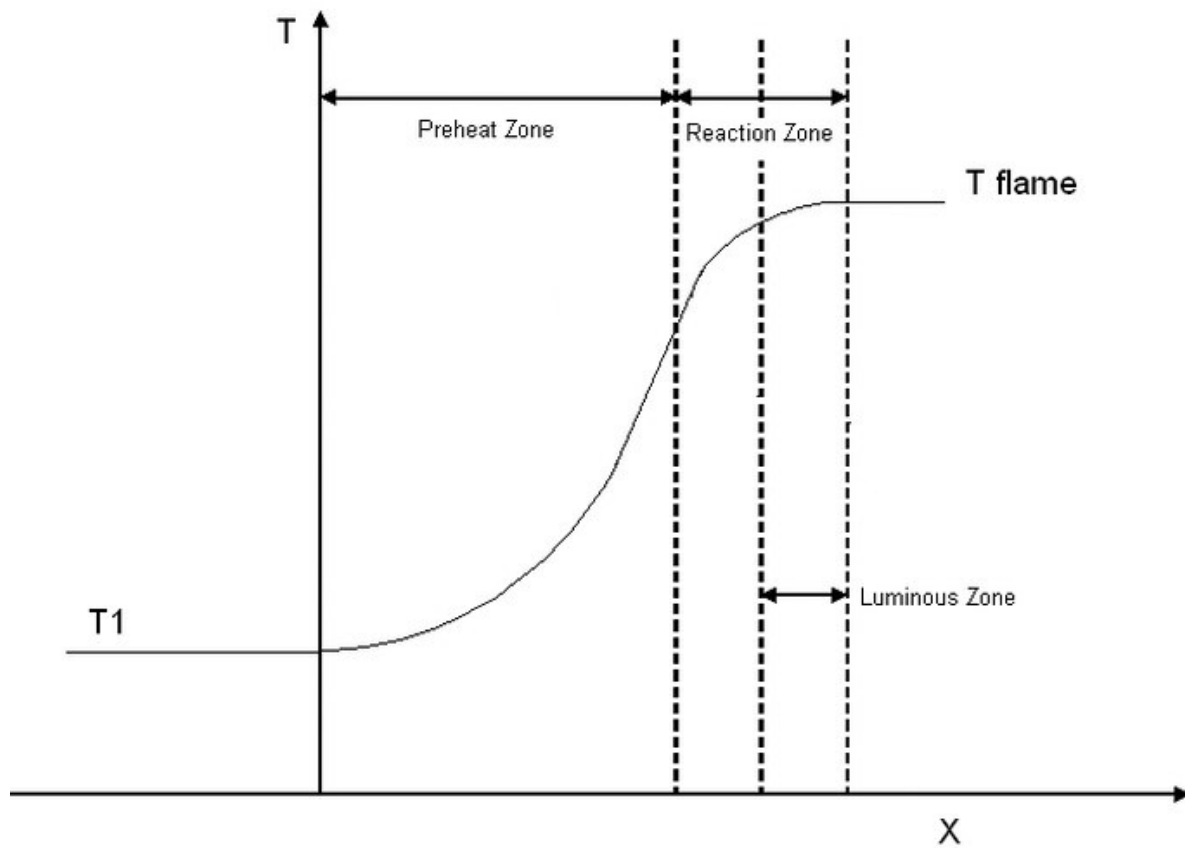
Figure 3 *Premixed Flame Structure*

2.5 Extinction and Ignition curve, S-Curve

It is shown that also for premixed flames, the S-curve (by Linan [20] for diffusion flames) describes the burning limits over the maximal temperature. [19]

The S-curve shown in Figure 4 shows the strain rate [1/s] (which defines the flow velocity) over the maximum flame temperature, T_{max} [K]. The curve has three different areas:

- Burning flame area (or upper branch)
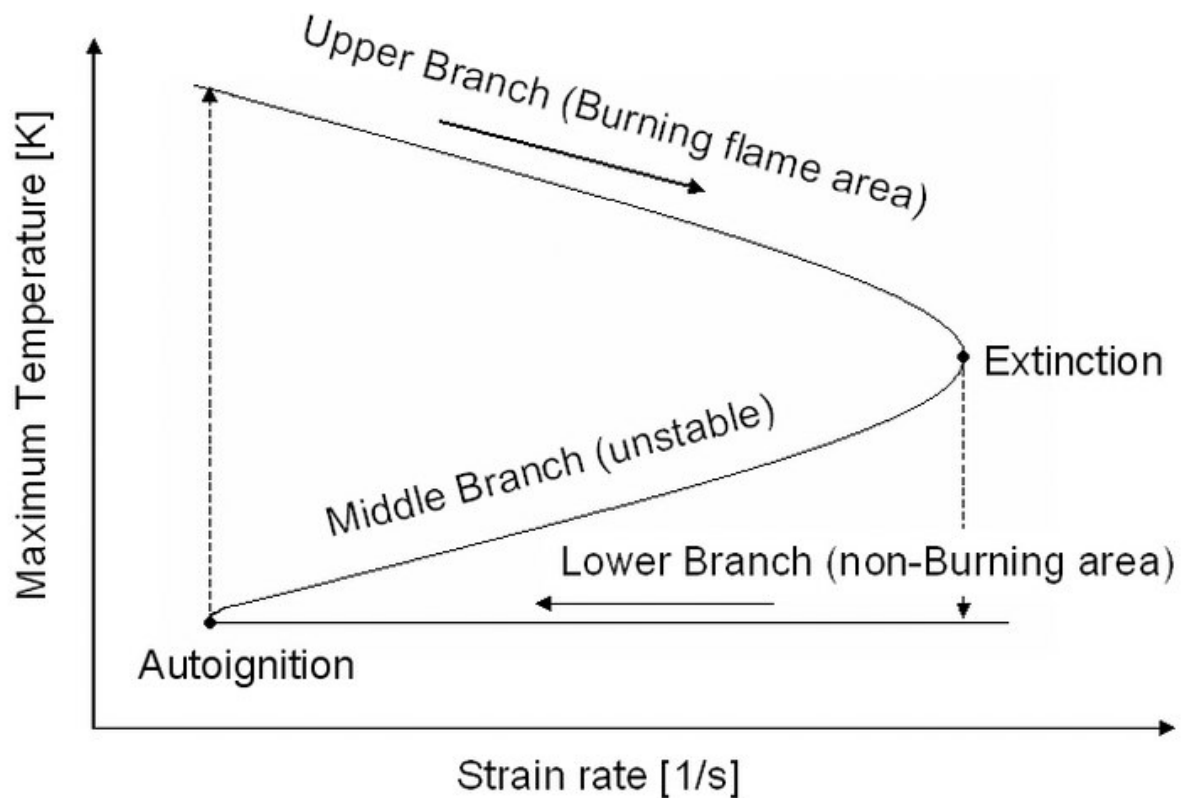- An unstable area (or middle branch)
- Non-burning area (or lower branch)

Figure 4 *S-curve*

The strain rate describes here the time, the reactants need to compose a reactant mixture. This time is called residence time. When increasing the strain rate, the reaction time decreases, so that at some point a non-reactive mixture is reached.

Burning flame area

By increasing the strain rate, the temperature decreases along the burning-area line due to the decrease of the residence time. At some point the residence time is so low that the reactants can't form a reactive mixture anymore. This point is called the extinction point. At that point the temperature drops from the burning area to a temperature on the non-burning area.

Non-burning area

On the line of the non-burning area at a high strain rate no flame can be reached due to the low residence time. By decreasing the strain rate along the non-burning area line, the residence time increases again until the ignition point is reached. At that point a flame occurs and the flame temperature jumps from the non-burning area up to a temperature on the burning area line. On the auto ignition point, the residence time is high enough again for building a reactive mixture.

Unstable area

This is a physically unstable area and can never been reached.

3. Experimental Apparatus

3.1 Counter flow configuration

The experiments are carried out in a counter flow configuration, where a premixed flame is stabilized between two axis symmetric ducts at a pressure of p = 1.013 [bar]. The counter flow configuration consists of a burner with 2 ducts, a lower duct with assigned index 1 and an upper duct with an assigned index 2. The distance between the two ducts is L = 10 [mm] for extinction experiments. An inert gas stream of nitrogen coming from the top (duct 2) is injected in a fuel/oxygen/nitrogen mixture coming from the lower duct 1. The two laminar flow streams build a stagnation plane between the ducts. At that point the velocities are considered to be zero. V_2 and T_2 represent the flow velocity and the temperature at the exit of the duct of the pure nitrogen stream of duct 2. The properties of the mixture from duct 1 are given by the velocity V_1, the temperature T_1, fuel-air ratio Φ and oxygen mass fraction Y_{ox}. The experiments were carried out for $T_1 = 483$ [K] (210 [°C]) ± 5 [K], $T_2 = 298$ [K] (25 [°C]), $Y_{ox} = 0.18$, and Φ usually from 0.9 to 1.225. Both flows are considered to be plug flows, what means that the flows have no tangential components at the exit of the ducts. The position of the flame is always below the stagnation plane due to the fuel coming from the lower duct. The position of the stagnation plane changes during the experiments because only V_2 is changed when running the experiments and V_1 stays constant for the same Φ, thus, there is no mass balance between both streams: $\rho_1 \cdot V_1^2 \neq \rho_2 \cdot V_2^2$ like it is in non-premixed experiments. The velocity V_1 of the fuel stream must always be greater than the laminar burning velocity, to prevent flashback. Figure 5 shows the counter flow configuration with duct 1 and duct 2.
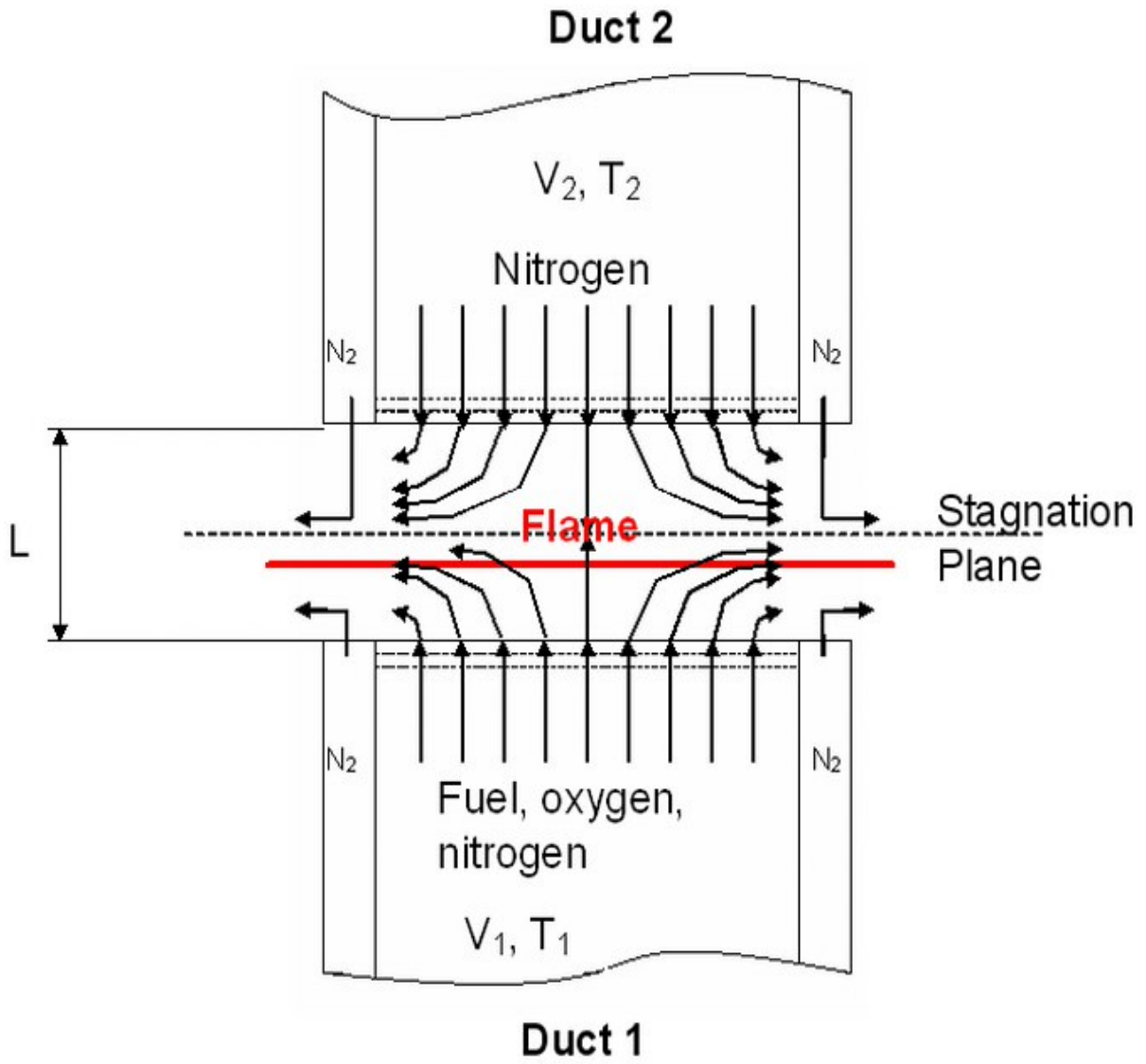
Figure 5 *Counter flow configuration*

The reactant stream coming from duct 1 is represented by the strain rate a_1 and is defined as gradient of the normal component of the flow velocity. [21]

The strain rate a_1 is given by [21]:

$$a_1 = \frac{2|V_1|}{L}\left(1 + \frac{|V_2|\sqrt{\rho_2}}{|V_1|\sqrt{\rho_1}}\right)$$

Where a_1 [s^{-1}] is the strain rate of the fuel side, L [m] is the distance between the two ducts, V_i [m s^{-1}] are the flow velocities and ρ_i [kgm^{-3}] are the densities. The inert side is given by index 2 and the fuel side by index 1.

The strain rate for the inert side a_2 is given by [21]:

$$a_2 = \frac{2|V_2|}{L}\left(1 + \frac{|V_1|\sqrt{\rho_1}}{|V_2|\sqrt{\rho_2}}\right)$$

The accuracy of the strain rate values is ± 10 % of the recorded value and that of the fuel mass fraction and oxygen mass fraction ± 3 % of the recorded value. The experimental repeatability on reported strain rate is ± 5 % of recorded value.

3.2 Experimental setup

The experimental setup is shown in Figure 6. It consists of:

- vaporizer,
- burner (duct 1 and duct 2),
- syringe pump for the fuel supply,
- exhaust system,
- gas bottles (oxygen and nitrogen),
- heating tapes,
- heating plate,
- mass flow controllers,
- thermocouples,
- computer control system.

The fuel is pumped from the syringes to the preheated vaporizer. The fuel enters the vaporizer through a spray nozzle. Inside the vaporizer, the fuel gets vaporized and mixed with nitrogen. The temperature in the vaporizer is around 483 [K] (210 [°C]) ± 5 [K] which is higher than the required boiling temperature of all tested fuels which must at least be reached for complete vaporization. The vaporized fuel/nitrogen mixture exits the vaporizer through heated

lines and gets mixed with oxygen immediately after exiting the vaporizer. The vaporized fuel/oxygen/nitrogen mixture flows further to the lower part (duct 1) of the burner where it exits the duct and streams against a pure nitrogen stream coming from the upper part of the burner (duct 2).

Thermocouples (Omega, Type E: Chromega®/Constantan) in the vaporizer and in duct 1 measure the temperature of the fuel/nitrogen mixture in the vaporizer and the vaporized fuel/oxygen/nitrogen stream in duct 1.
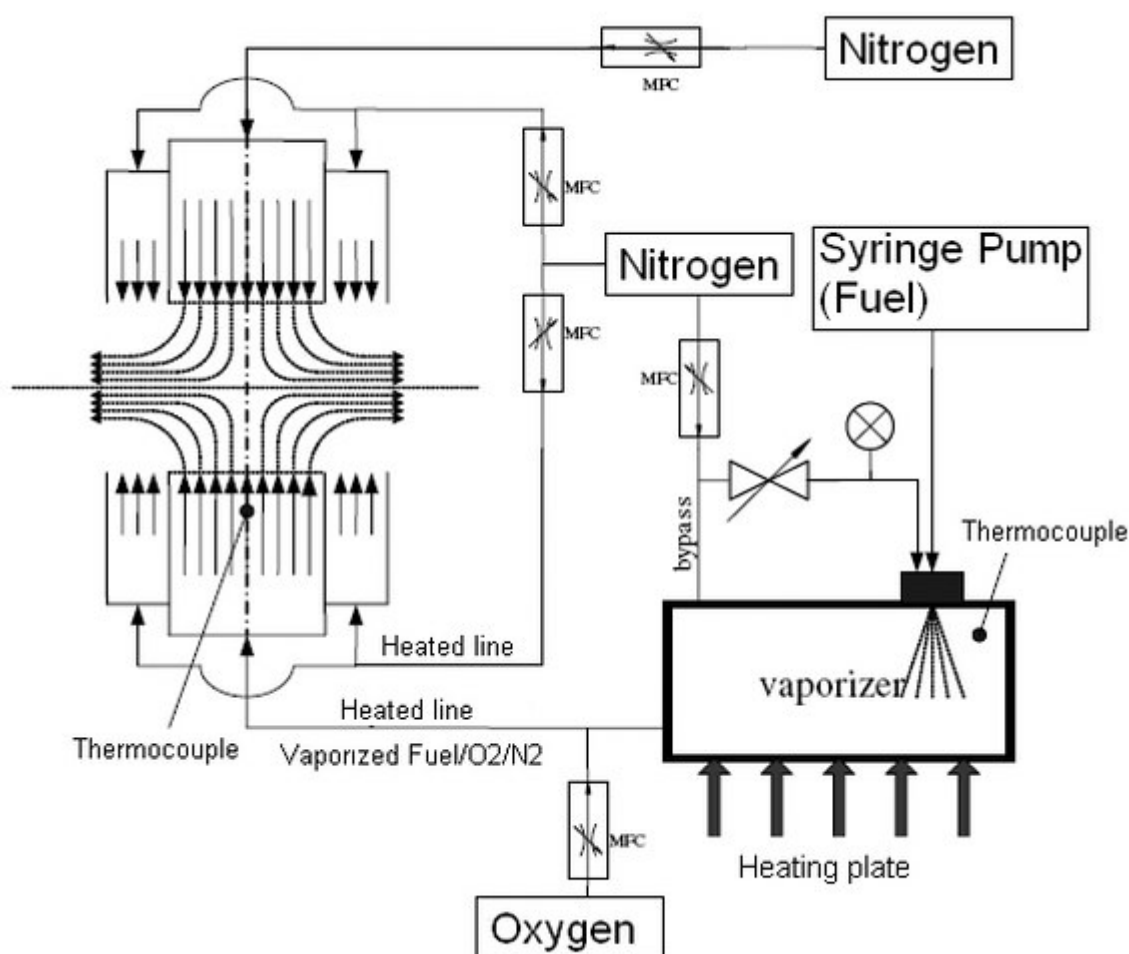
Figure 6 *Schematic illustration of the experimental setup*

3.2.1 Gas Supply

The gas supply is given by compressed nitrogen and oxygen bottles.
Nitrogen is used:

- as curtain, to avoid reactions with the ambient air
- as inert gas (stream from duct 2)
- to vaporize the fuel
- for the fuel/oxygen/nitrogen mixture.

The computer program which controls the gas flow is written in C++. When opening the program, a graphical user interface appears where all the data like: strain rates of the inert side, Φ, mass fraction Y_{ox} (here $Y_{ox} = 0.18$), curtain velocities, fuels, distance between the ducts and temperatures have to be entered. A screenshot of the program is shown in figure 7.
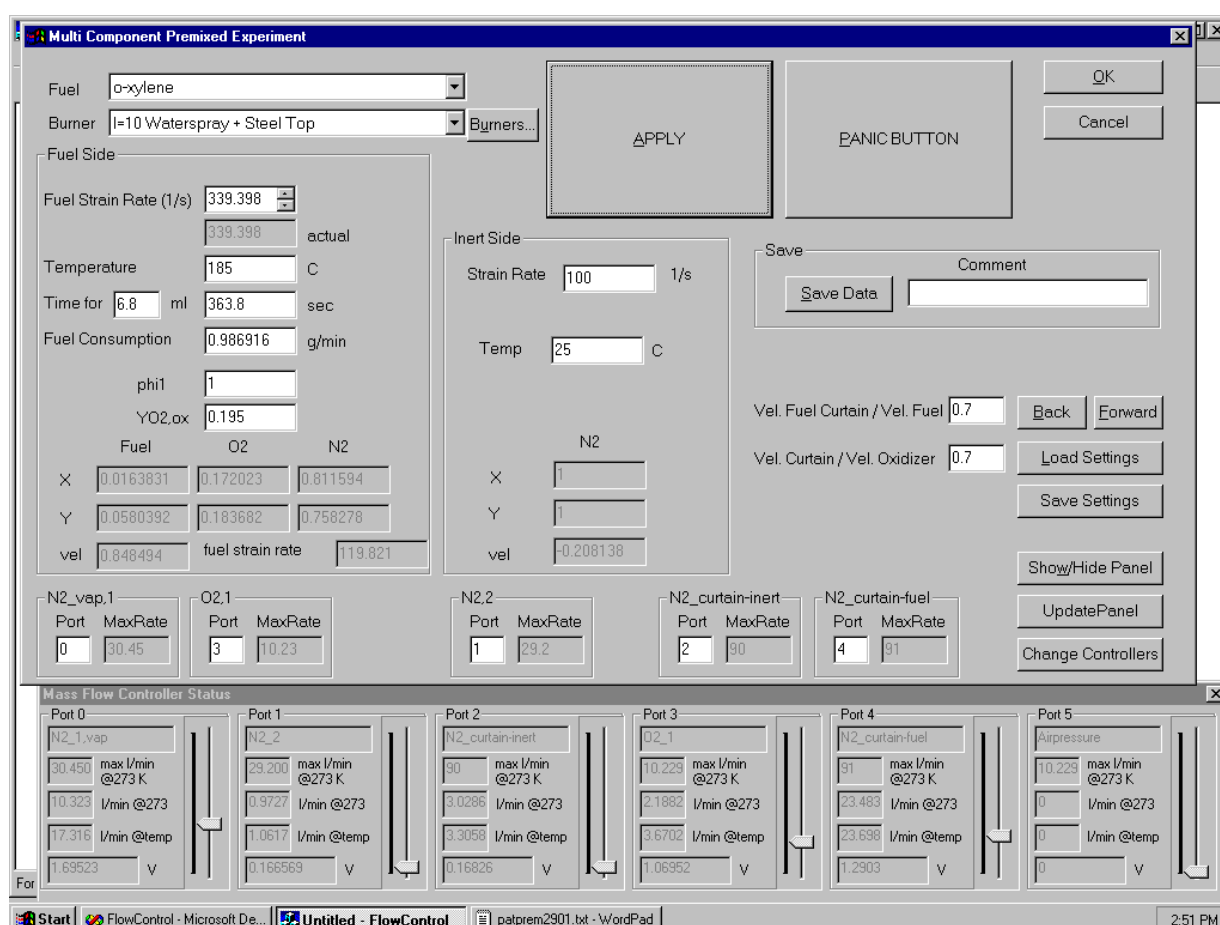

Figure 7 *Screenshot of the Counter flow setup computer program*

24

By providing the program with different strain rates and curtain velocities, the program is able to change those by sending different signals from (0 Volt to 5 Volt) to the flow controllers where 0 Volt means no flow and 5 Volt means maximum flow.

At the beginning of the experiments, all flow controllers must be calibrated. This is done by using a wet test meter (Petroleum Analyzer Company L.P.) which has to be hooked up to the different lines at a time. Then the time is taken for 30 liter gas. With this time and the time given by the computer program the new flow rate can be calculated and be changed in the program. This is an iterative process and is repeated until an accord of less than 1%.

3.2.2 Fuel supply

The fuel supply is given by a syringe pump (Harvard Apparatus, Model 975 which is shown in Figure 8) the fuel speed can be adjusted by switching gears on the pump. When switching gears, the amount of fuel that is going into the vaporizer must also be changed in the computer program. The experiments were all run at gear 12, which means 6.8 [ml] fuel in 363.8 seconds with two 20 [cc] syringes.
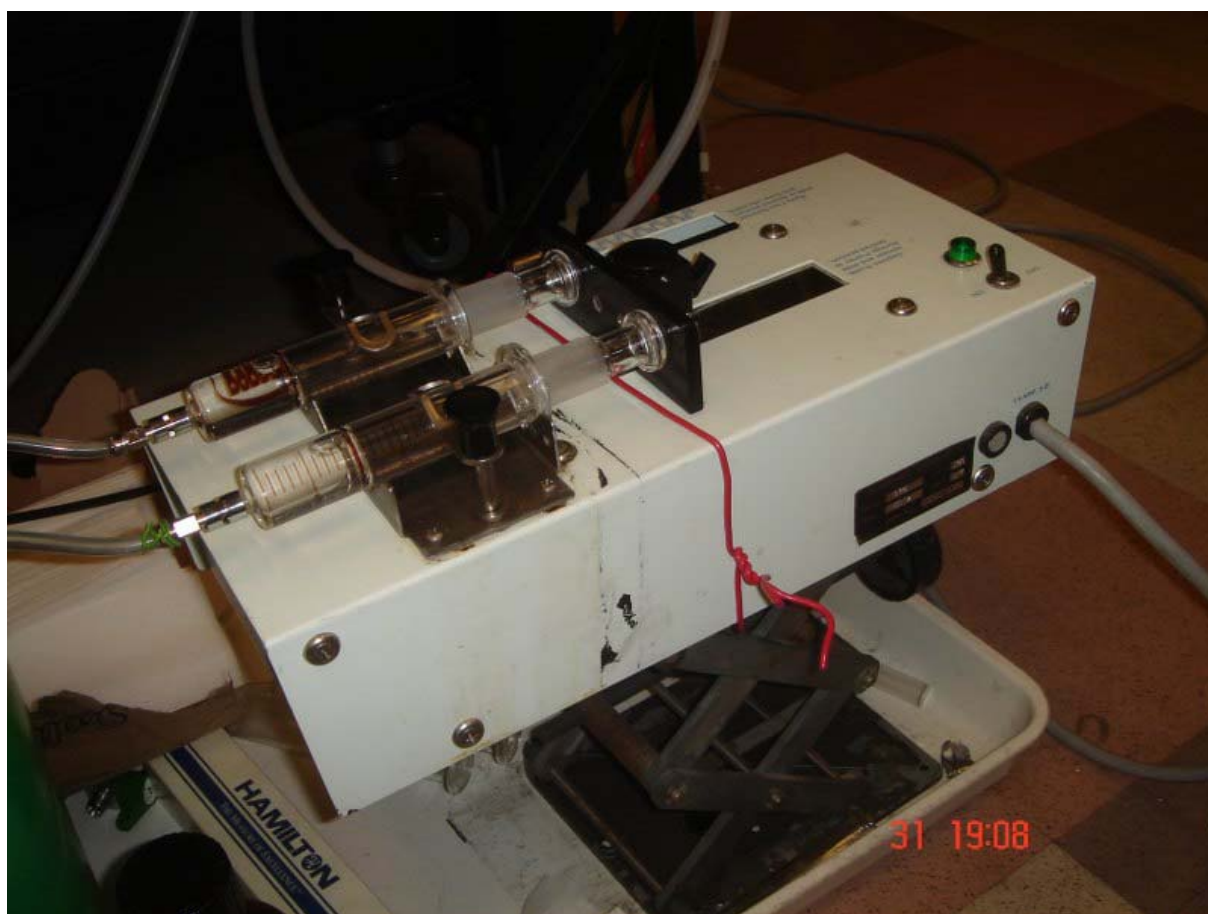
Figure 8 *Photo of the fuel pump with syringes*

3.2.3 Exhaust system

Cooling water, hot exhaust and soot are removed via a vertically mounted separator. The exhaust system has one inlet and two outlets. The liquids quit the separator at the bottom through a disposal line. The gases quit the separator at the top through the suction, like shown in figure 9.
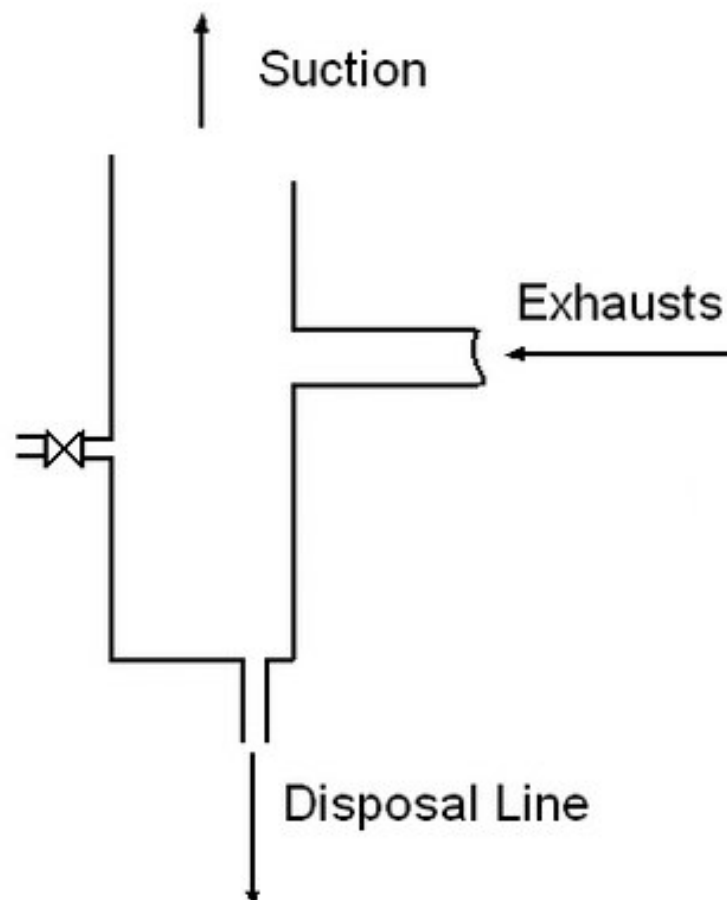
Figure 9 *Sketch of the exhaust system*

3.2.4 Burner

The burner is a complex aluminum construction which consists of an upper and a lower part. Figure 10 shows a cross section. [22]
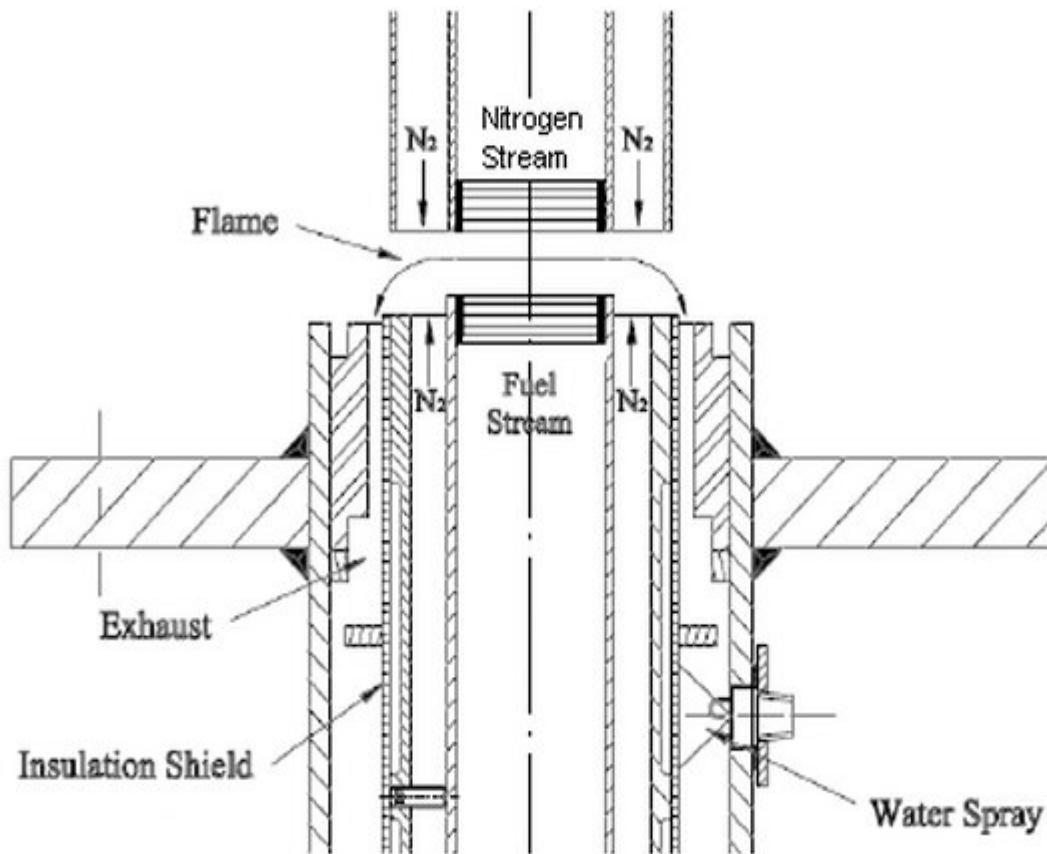
Lower part of the burner

The lower part consists of three different aluminum tubes:

1. The <u>fuel duct</u> (d_{fuel} = 24 mm) bears the fuel/oxygen/nitrogen mixture and is the center of the lower part. 3 stainless steel screens (Type: 200m-0021; diameter 1.45 inch) are mounted to the end of the fuel duct each separated by a stainless steel ring. A thermocouple is mounted in that tube to measure the temperature of the mixture.

2. The <u>curtain duct</u> ($d_{curtain}$ = 40 mm) surrounds the fuel duct and bears the nitrogen curtain. The curtain is there, to avoid chemical reactions between the ambient air and the fuel mixture.

3. The <u>exhaust duct</u> ($d_{exhaust}$ = 60 mm) surrounds the curtain duct. The exhaust duct is holding 8 water spray nozzles for cooling the hot exhaust to avoid auto ignition.

Upper part of the burner

The upper part of the burner is an assembly consisting of a smaller tube of 22 mm surrounded by a larger duct of 57 mm. The smaller tube or duct contains the pure nitrogen stream which is directed towards the fuel mixture stream. 3 stainless steel screens (Type: 200m-0021; diameter 1.45 inch) are mounted at the end of the tube and are separated by stainless steel rings. The larger tube bears the nitrogen curtain to avoid reactions with the ambient air.

Figure 10 *Cross section of the Burner (upper part and lower part).* [22]

3.2.5 Spray Vaporizer

The vaporizer is a 220 x 150 x 120 mm aluminum box. The fuel is pumped from two syringes into the vaporizer, where it's sprayed in through a nozzle using nitrogen as a carrier gas. The vaporizer is heated by a heating plate from the bottom and is surrounded by insulation to avoid condensation. A nitrogen stream takes the vaporized fuel out of the vaporizer. The vaporized fuel/nitrogen mixture exits the vaporizer and is mixed outside of the vaporizer with oxygen. This fuel/oxygen/nitrogen mixture flows through heated lines to the burner. Water cooling avoids overheating of the vaporizer.

4. Experimental approach

Before starting with the experiments the 3 screens have to be mounted inside the two ducts. The upper part of the burner (duct 2) has to be put on the lower part and adjusted using 3 screws. Next, the heating plate and tapes must be switched on and adjusted to reach the desired temperature. The desired temperatures are reached after approximately 45 minutes of heating. The distance L between both ducts has to be checked again and adjusted because of material expansion due to heating.

The next step is to open the valves on the flow controller panel; this has to be done very carefully in order to prevent damage to the flow meters. The syringes have to be filled up with the desired fuel and the cooling water has to be opened via a valve.

Next step is to select the right setting in the mass flow controller program. This is for premixed experiments the "multi component setting". The setting with all its features appears then in the computer program. The program has to be provided with the right fuel, the distance L between the ducts, the time for 6.8 ml fuel (what means gear 12), Y_{ox}, starting Φ, and starting inert side strain rate a_2. Gear 12 has to be chosen on the fuel pump, which has to be switched on. The starting point for Φ and inert side strain rate were usually around 0.9 respectively 150 [1/s]. When changing the inert strain rate, the fuel strain rate is automatically changed as well. The fuel usually needs a couple of minutes to reach the inlet of the vaporizer and then it takes a short time for getting vaporized before the desired fuel/oxygen/nitrogen mixture is reached. This time delay also happens when refueling the syringes or changing Φ. Therefore it is always important to wait a couple of minutes after these changes, before continuing with the experiments. When the mixture has reached the exit of duct 1, this mixture is lighted up by using a blow torch. Once the mixture burns, the inert side strain rate a_2 is increased in steps of 2 [1/s] until extinction is observed. After extinction, it has to be tried to ignite the mixture again at the same strain rate because it was found out that for these kinds of premixed flames experiments, extinction sometimes happens at a strain rate where it shouldn't occur. When the final extinction is reached, the strain rate point can be saved. After that, the next Φ is entered in the program. Φ is changed in steps of 0.025 until a final Φ of 1.225 or 1.25 is reached, depending on the starting point and the peak of the different fuels. At least 3 runs for each fuel have to be done. Figure 11 shows a JP-8 flame.

Premixed reactant Stream: JP-8/Oxygen/Nitrogen Φ = 0.9, Y_{ox} = 0.175, T_1 = 463 [K] (210 [°C]), Inert Stream: Nitrogen, T_2 = 298 [K] (25 [°C]), a_1 = 335 [1/s]. [23]

Figure 11 *Photo of a JP-8 flame*

5. Experimental results

5.1 Aliphatics

Figure 12 shows the experimental results of extinction for the three alkanes, n-Heptane, n-Decane, and n-Dodecane and the cycloalkane, Methylcyclohexane tested in this study. The fuel strain rate at extinction a_1 is plotted in a range over 200 [1/s] to 500 [1/s] as function of the equivalence ratio Φ. The symbols are the average results from the different measured runs. A flame can never occur at any point above the curve, because this is the non-burning area of the s-curve. The region (burning flame area, s-curve) below the lines is the region where flames occur; this is the area of a strain rate a_1 lower than the strain rate at extinction $a_{1,e}$. In the region above the curves, the strain rate is too high which means that the residence time is too low and the temperature drops from the burning area to the no burning area in the S-curve. The strain rates at extinction increase for all species with increasing Φ and reach their maximum at $\Phi = 1.15$. And after that point the strain rate goes down again. This can be explained by the fact that the flame temperature reaches its maximum at $\Phi > 1$ due to the excess of fuel. It drops again after reaching its peak due to the lack of oxygen. At $\Phi < 1.15$ the temperature drops and so does the extinction curve due to the excess of oxygen. This ends in flame failures.
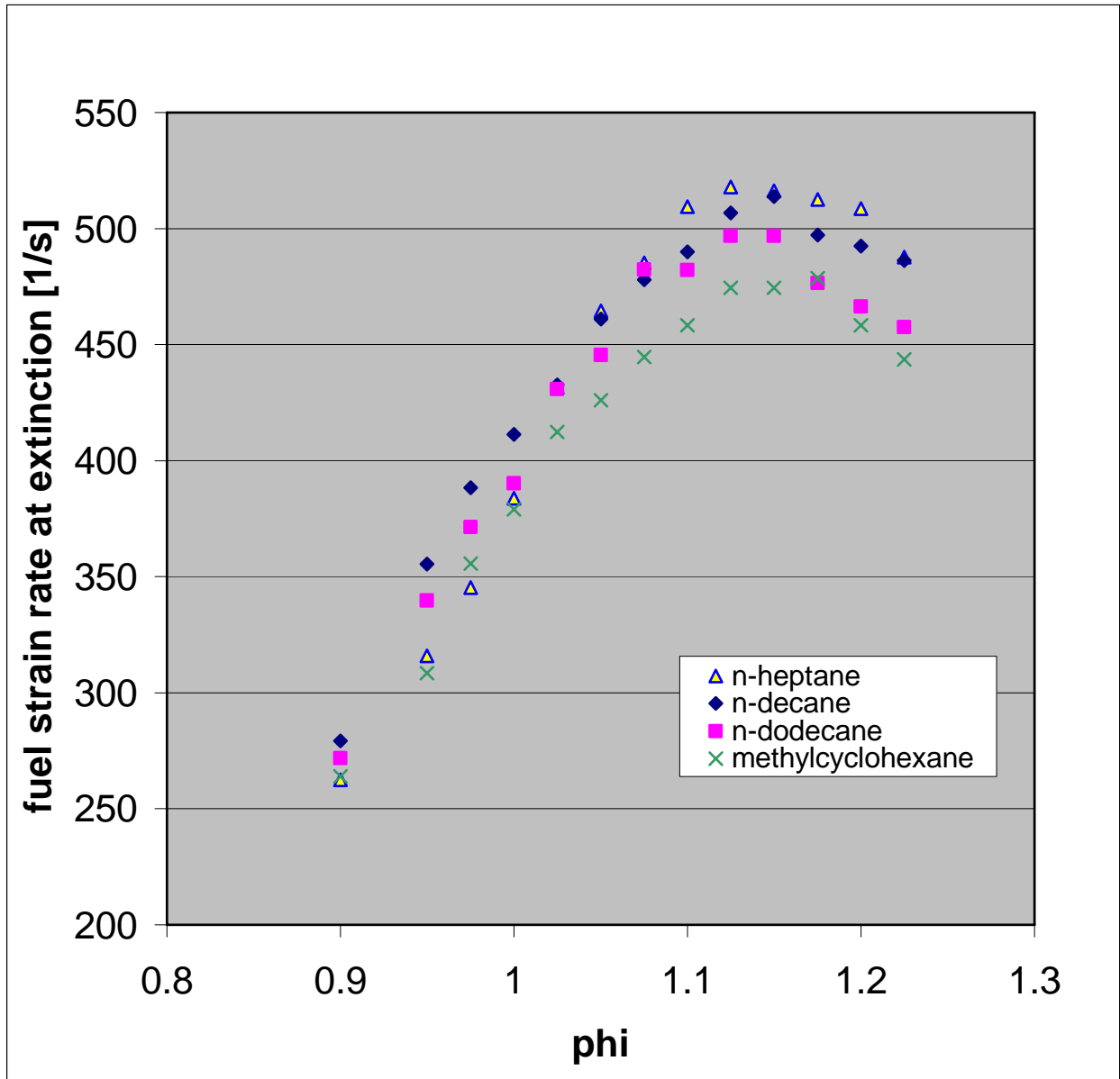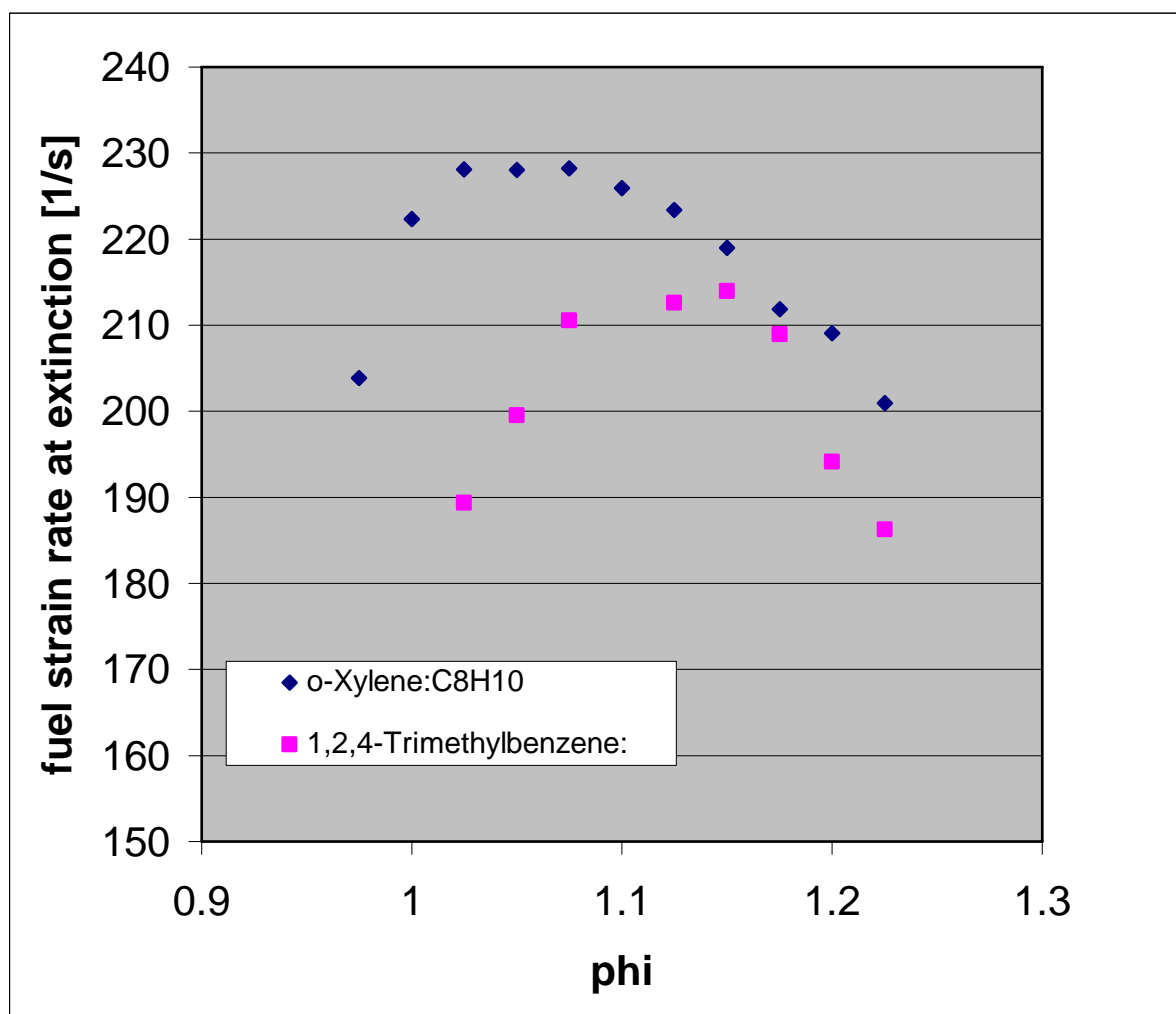
Figure 12 *Comparison of the fuel strain rate at extinction [1/s] over Φ for the 3 Alkanes and the Cycloalkane at Y_{ox} = 0.18. The fuel mixture temperature T_1 = 483 [K] (210 [°C]) ± 5 [K] and the inert side temperature T_2 = 298 [K] (25 [°C]).*

5.2 Aromatics

Figure 13 shows the two aromatics (o-Xylene and 1,2,4-Trimethylbenzene) tested in this study. The fuel strain rate at extinction (in a range of 150 [1/s] to 240 [1/s]) is plotted as function of the equivalence ratio Φ (in a range of 0.9 to 1.3) for the experimental results. Extinction is reached above the curves. o-Xylene reaches a higher maximum fuel strain rate (230 [1/s]), which means that 1,2,4-Trimethylbenzene (maximum fuel strain rate 212 [1/s]) is

easier to extinguish than o-Xylene. The curves of both fuels look similar. The maximal strain rate for o-Xylene is between a Φ of 1 to 1.15 and for 1,2,4-Trimethylbenzene between 1.075 to 1.175. From $\Phi = 1.1$ to 1.225 the maximal fuel strain rate at extinction is pretty much the same. Below $\Phi = 1.1$ o-Xylene seems to be more reactive than 1,2,4-Trimethylbenzene and therefore reaches a higher fuel strain rate at extinction. Furthermore, the lowest Φ for o-Xylene is at 1.025 and for 1,2,4-Trimethylbenzene at 0.975.

Figure 13 *Comparison of the fuel strain rate at extinction [1/s] over Φ for the unsaturated hydrocarbons, o-Xylene and 1,2,4-Trimethylbenzene at $Y_{ox} = 0.18$. The fuel mixture temperature $T_1 = 483$ [K] (210 [°C]) ± 5 [K] and the inert side temperature $T_2 = 298$ [K] (25 [°C]).*

5.3 JP-8 and Surrogates

Figure 14 shows the fuel strain rate at extinction over the equivalence ratio Φ for JP-8, Surrogate C, and Aachen Surrogate (components of the surrogates are given in table 1) at Y_{ox} = 0.18. The fuel strain rates are plotted from 200 [1/s] to 400 [1/s] and the equivalence ratio Φ from 0.8 to 1.3. The curves for all three fuels have the same trend. The fuel strain rates increase with increasing Φ, to a maximal fuel strain rates at around 380 [1/s] at a Φ around 1.15. After reaching their peaks, the fuel strain rates drop again. Both surrogates agree well with JP-8 especially on the rich side where the maximum fuel strain rates are reached. Above the lines, the residence time is too low so that the flame extinguishes. Thus, above the lines the non burning area on the s-curve is reached and the burning area is below the lines. Aachen Surrogate is slightly closer to JP-8 than Surrogate C.
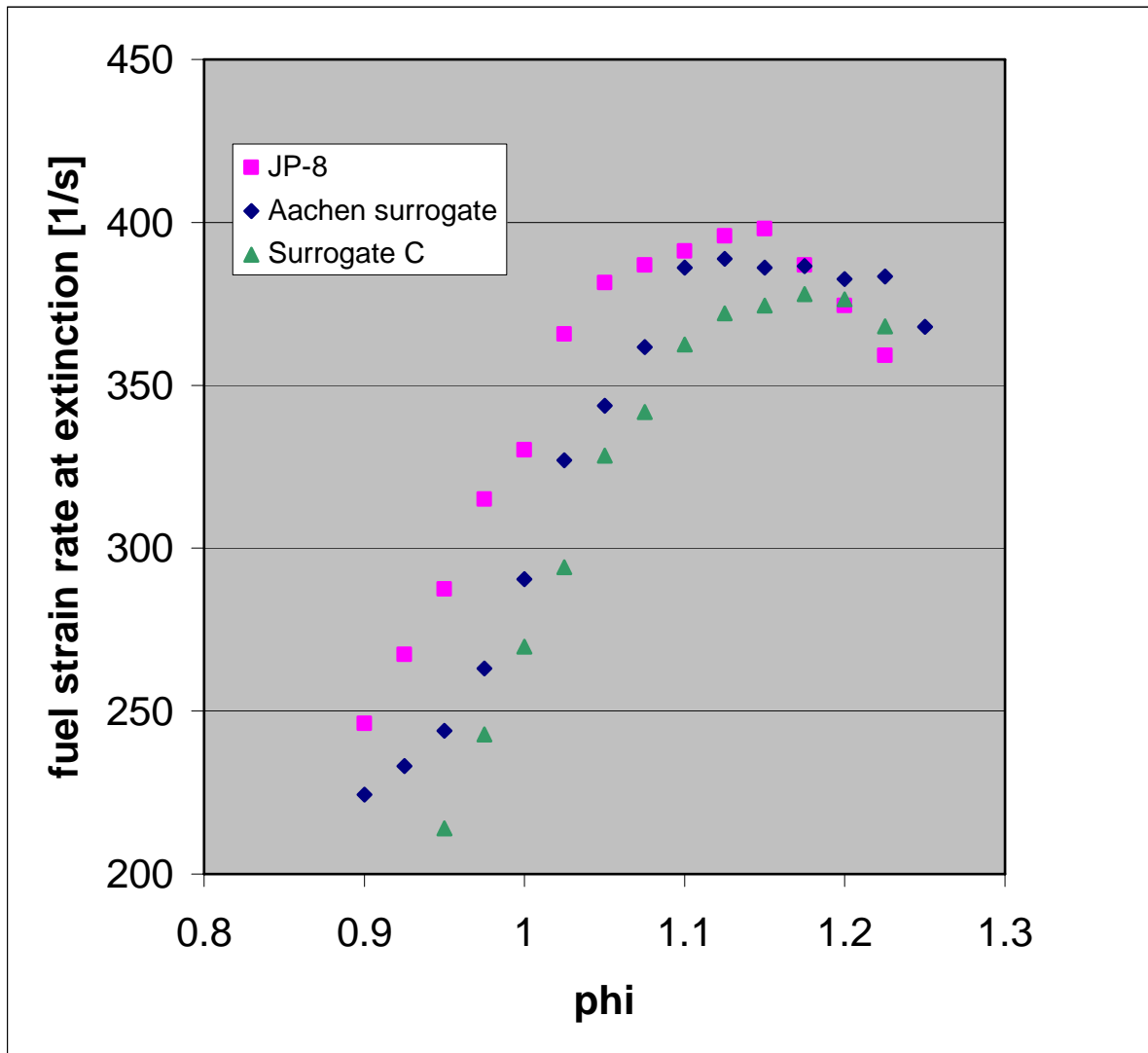
Figure 14 *Comparison of the fuel strain rate at extinction [1/s] over Φ for JP-8 and the Surrogates at Y_{ox} = 0.18. The fuel mixture temperature T_1 = 483 [K] (210 [°C]) ± 5 [K] and the inert side temperature T_2 = 298 [K] (25 [°C]).*

## 5.4 Surrogates and their components

In Figure 15, the Surrogate C, his components n-Dodecane, Methylcyclohexane, and o-Xylene are shown in blue and Aachen Surrogate with its components n-Decane and 1,2,4-Trimethylbenzene are shown in red dots. The graph shows the fuel strain rate at extinction [1/s] over the equivalence ratio Φ. The fuel strain rate is plotted from 150 [1/s] to 550 [1/s] and Φ from 0.8 to 1.3. The surrogates are located between their alipahtic and aromatic components, thus, in an area where they are expected to be.
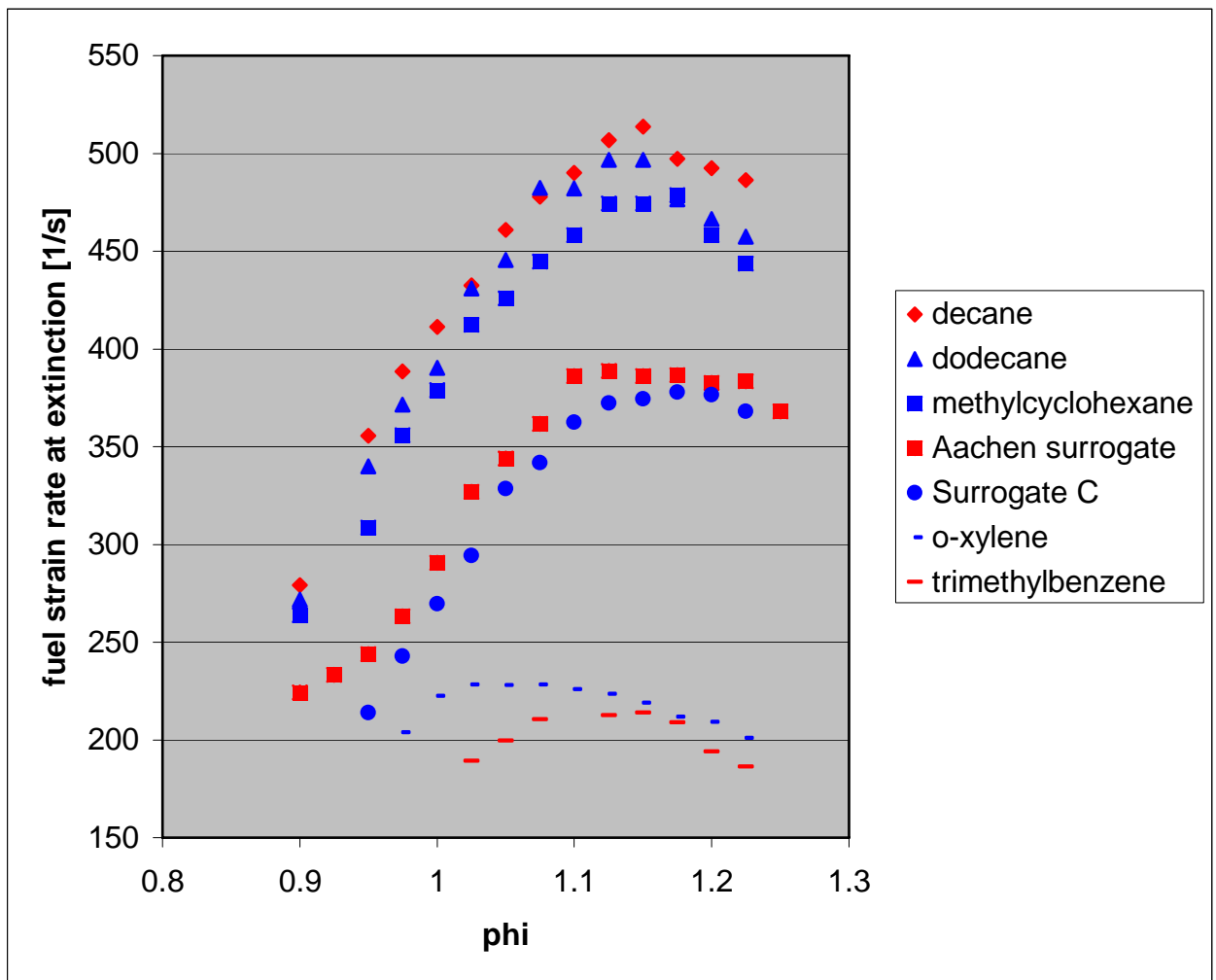
Figure 15 *Comparison of the fuel strain rate at extinction [1/s] over Φ for the tested Surrogates and their components at Y_{ox} = 0.18. The fuel mixture temperature T_1 = 483 [K] (210 [°C]) ± 5 [K] and the inert side temperature T_2=298 [K] (25 [°C]).*

35

5.5 All experimental measured fuels

Figure 16 shows all the experimental results for the tested fuels in one graph with fuel strain rate at extinction as function of equivalence ratio Φ. The fuel strain rate is plotted from 150 [1/s] to 550 [1/s] and Φ from 0.8 to 1.3. JP-8 and the surrogates have their maximal fuel strain rates between the aromatics and aliphatics. The fuel strain rate at extinction difference between the aliphatics and aromatics can be seen. The fuel strain rate difference between the aliphatics and 1,2,4-Trimethylbenzene is approximately 225 [1/s] for all Φ. Due to the flat curve of o-Xylene the strain rate difference varies from 180 [1/s] in the region of $\Phi = 1$ to 225 [1/s] above $\Phi = 1.1$. This shows that the aromatics are less reactive than the aliphatics due to their benzene ring structure what was predicted in the theory part. A higher energy is needed to break the ring down.
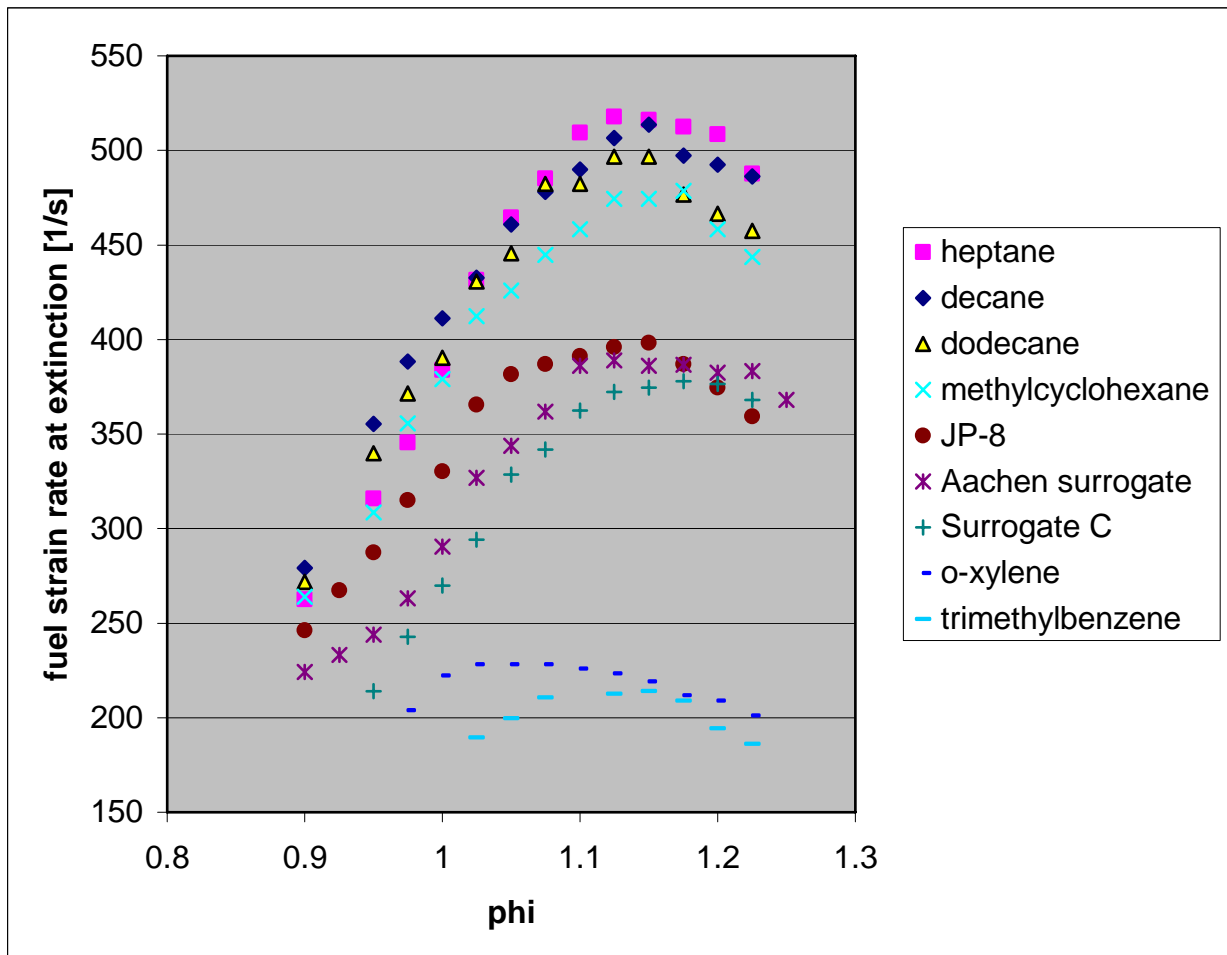
Figure 16 *Comparison of the fuel strain rate at extinction [1/s] over Φ for JP-8, the Surrogates and all of the Hydrocarbon Fuels at $Y_{ox} = 0.18$. The fuel mixture temperature $T_1 = 483$ [K] (210 [°C]) $\pm$ 5 [K] and the inert side temperature $T_2 = 298$ [K] (25 [°C]).*

5.6 Experimental and numerical results for n-Decane and o-Xylene

Figure 17 shows the numerical calculation (see paragraph 6.1) by Alessio Frassoldati and coworkers (Politecnico di Milano, Dipartimento di Chimica) and the experimental results for n-Decane and o-Xylene. The fuel strain rates at extinction are plotted as function of the equivalence ratio Φ. The fuel strain rates are plotted in a range of 100 to 700 [1/s] and the equivalence ratio Φ in a range of 0.8 to 1.3. The numerical data are represented by straight lines and the experimental data by dots. Above the lines is extinction and flames are below the lines.
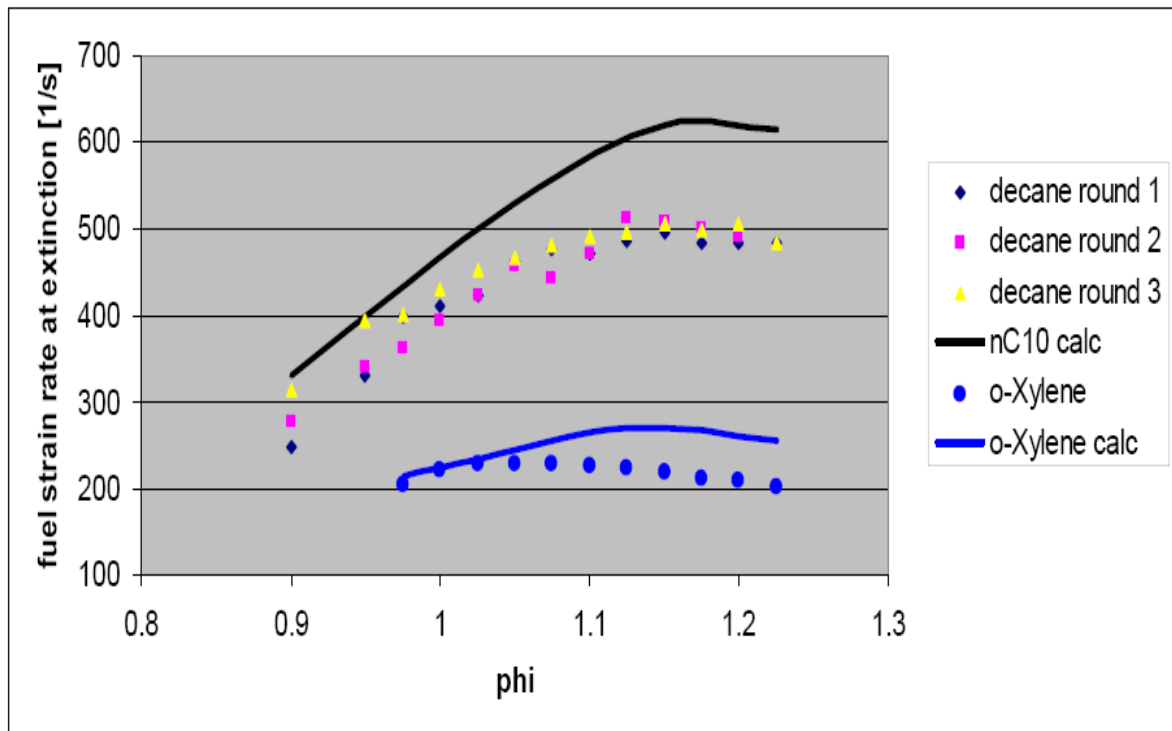
Figure 17 *Comparison of the fuel strain rate at extinction [1/s] over Φ for n-Decane and o-Xylene at Y_{ox} = 0.18. The graph shows the experimental results in dots and the numerical result in straight lines. The fuel mixture temperature T_1 = 483 [K] (210 [°C]) ± 5 [K] and the inert side temperature T_2 = 298 [K] (25 [°C]).*

n-Decane

For n-Decane, the three measured rounds and the numerical result are shown in the graph. The experimental and the numerical results show similar behavior, the fuel strain rate increases with increasing Φ, reach their maximums at around $\Phi = 1.15$ and decrease again. For the fuel strain rate, the experimental data agree very well with the numerical data for $\Phi = 0.9$ to 1.1. In the region of their maximums, the numerical data is slightly overpredicted compared to the experimental data with around a strain rate of 100 [1/s]. It was noticed during the experiments that the flame comes closer and closer to the outlet of duct 1 with increasing the strain rate.

o-Xylene

The numerical result (straight line) and the average experimental result (dotted line) of o-Xylene can be seen in the lower part of the graph. The data are taken from $\Phi = 0.975$ to 1.225 and for a fuel strain rate of 100 [1/s] to 700 [1/s]. The numerical and measured results agree very well with each other for all Φ. Both lines don't show real maximum fuel strain rate point, so no real peak. The maximum fuel strain rate at extinction is for the numerical result from $\Phi = 1.125$ to $\Phi = 1.175$ and for the experimental data from $\Phi = 1$ to $\Phi = 1.15$.
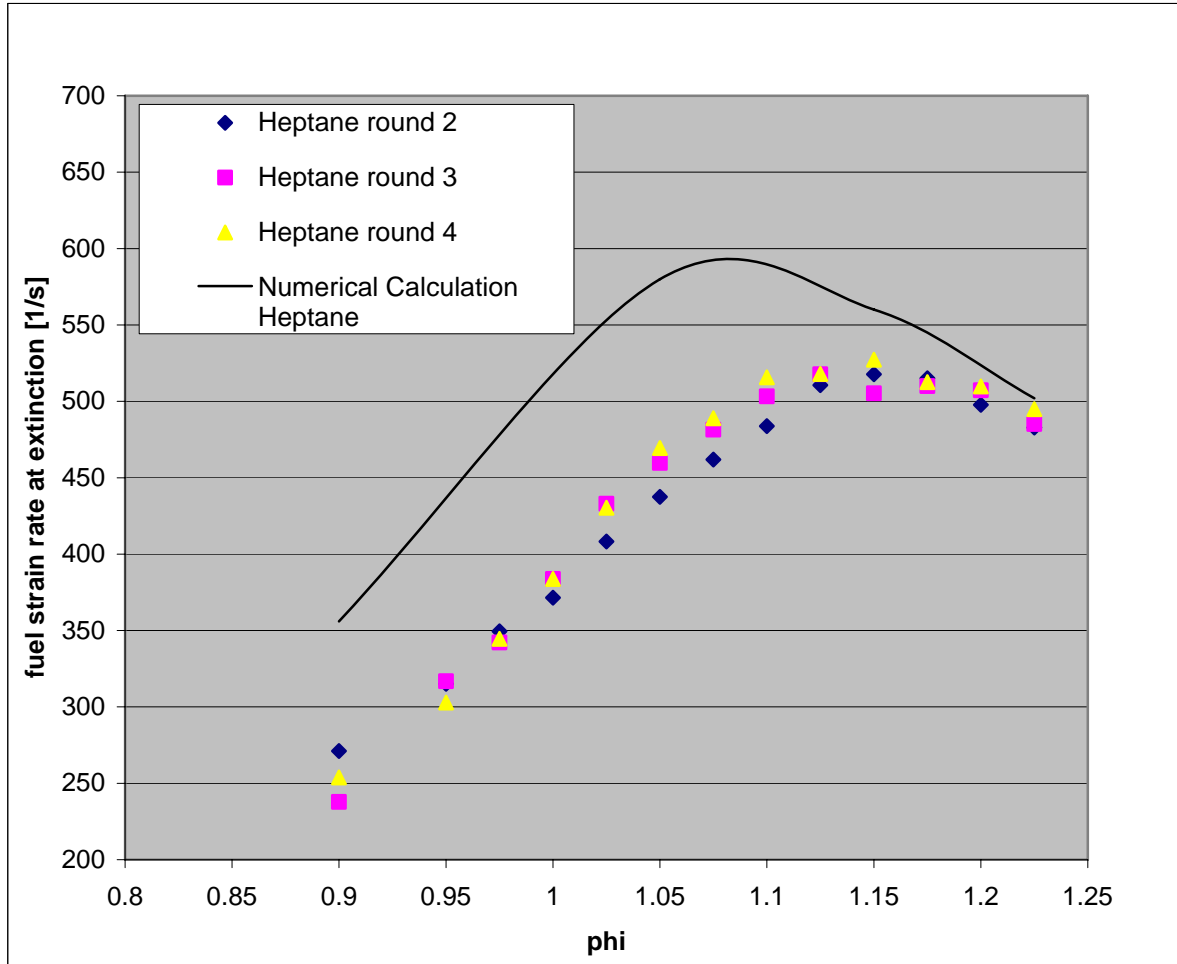
5.7 Experimental and numerical results for n-Heptane

Figure 18 shows the numerical and experimental results for n-Heptane. The graph is plotted as function of fuel strain rate over equivalence ratio Φ. The fuel strain rates are plotted in a range of 200 [1/s] to 700 [1/s] and the equivalence ratio Φ from 0.8 to 1.25. The numerical result is given as a line and the experimental results for 3 different runs in dots. The calculation was done using a reduced chemical mechanism with 159 species [24]. In Chemkin, a maximal number of grid points of 250 points were used.

The numerical curve reaches its maximum at a Φ of 1.075 and the experimental curve at Φ around 1.15. From $\Phi = 0.9$ to $\Phi = 1.1$ the chemical mechanism over predicts the experimental data of approximately 125 [1/s] fuel strain rates. In the region above $\Phi = 1.1$ the numerical and the experimental data agree very well. Thus, at lower Φ the result from the experiments

extinguish earlier than the numerical result. At higher Φ the numerical and the experimental data extinguish in the same region of fuel strain rate.

Figure 18 *Comparison of the fuel strain rate at extinction [1/s] over Φ for n-Heptane numerical and experimental at Y_{ox} = 0.18. The graph shows the experimental results in dots and the numerical result in a straight line. The fuel mixture temperature T_1 = 483 [K] (210 [°C]) ± 5 [K] and the inert side temperature T_2 = 298 [K] (25 [°C]).*

6. Numerical calculation

6.1 Numerical Approach

The numerical calculation is executed by using Chemkin 4.1.1., a computer program which is able to simulate combustion experiments like done in this study. The user can choose between several different reactors for simulating the desired calculations. For the premixed flame experiments the "premixed opposed-flow flame" reactor is used which accords with the counter flow setup used in the experiments. After choosing the reactor type, the program has to be provided by two inlet flows - one for the nitrogen and the other one for the fuel mixture. Furthermore, one outlet for the exhaust gases has to be chosen. These are the first steps which have to be taken.

The Pre-processor verifies the consistency and completeness of the chemistry sets and converts the chemical mechanism files into a binary form which is readable for Chemkin. The chemistry set for premixed flame simulation consists of a chemical mechanism, thermodynamic data, and transport data file. In the chemical mechanism all reaction for the problem are listed as well as additional information like activation energy and the frequency factor of each reaction. The Thermodynamic data are needed to calculate reaction rates. The Transport data gives information about convection, diffusion, and conductivity for the individual species. All species from the chemical mechanism must also be included in the transport and thermodynamic data. [25, 26]

The inputs for the fuel mixture and the nitrogen (species, flow velocities (strain rates), mass fractions, distance between both ducts, and temperatures) have to be entered. For the reactor, a pressure of 1 bar and 250 grid points were chosen. The Premixed Flame Model solves the set by calculating the chemical reaction rates with the given inputs.

The results and solutions from the calculation can be visualized in the Post-processor. The calculated values can be plotted from the Output Files or can be plotted in different graphs. To verify if there's a flame at the entered settings, the temperature profile can be plotted over the distance L between both ducts. A flame is simulated by a peak in the temperature file starting from T_1 and reaching T_2 after the peak, figure 19. The temperature for extinction just drops from T_1 to T_2, figure 19.
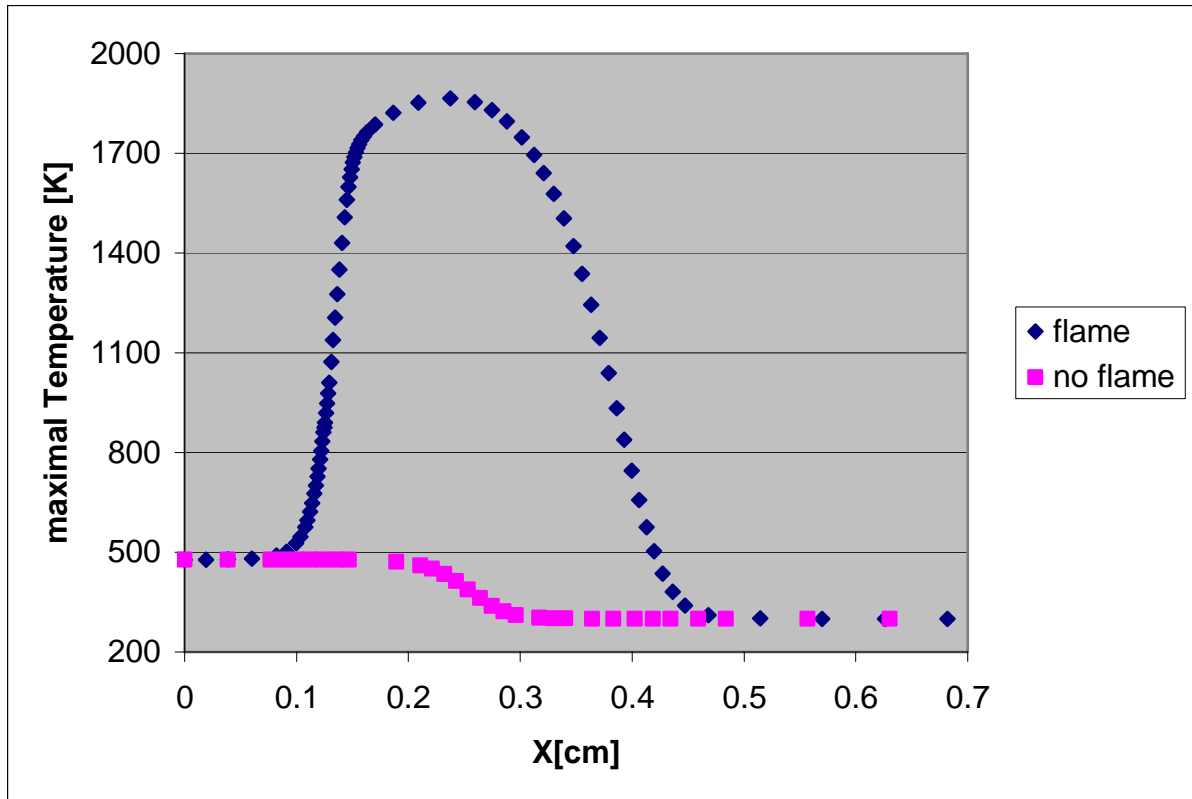
Figure 19 *The maximal Temperature over the distance between the two ducts for n-Heptane at $\Phi = 1.05$ with: $Y_{ox} = 0.18$, $\Phi = 1.05$, and a fuel strain rate of 475 [1/s] for a flame and 500 [1/s] for extinction. A flame is represented by the peak in the temperature and is shown in the figure in blue. It starts at the inlet temperature T_1 = 483 [K] (210 [°C]) ± 5 [K] at the exit of duct 1 where $x = 0$ [cm]. The Temperature drops again, after reaching its maximum temperature, to a temperature T_2 (duct 2) of 298 [K] (25 [°C]). Extinction is shown in pink. The temperature starts at T_1 and drops to T_2 in the region of the stagnation plane.*

6.2 Numerical results for n-Decane by Alessio Frassoldati and coworkers
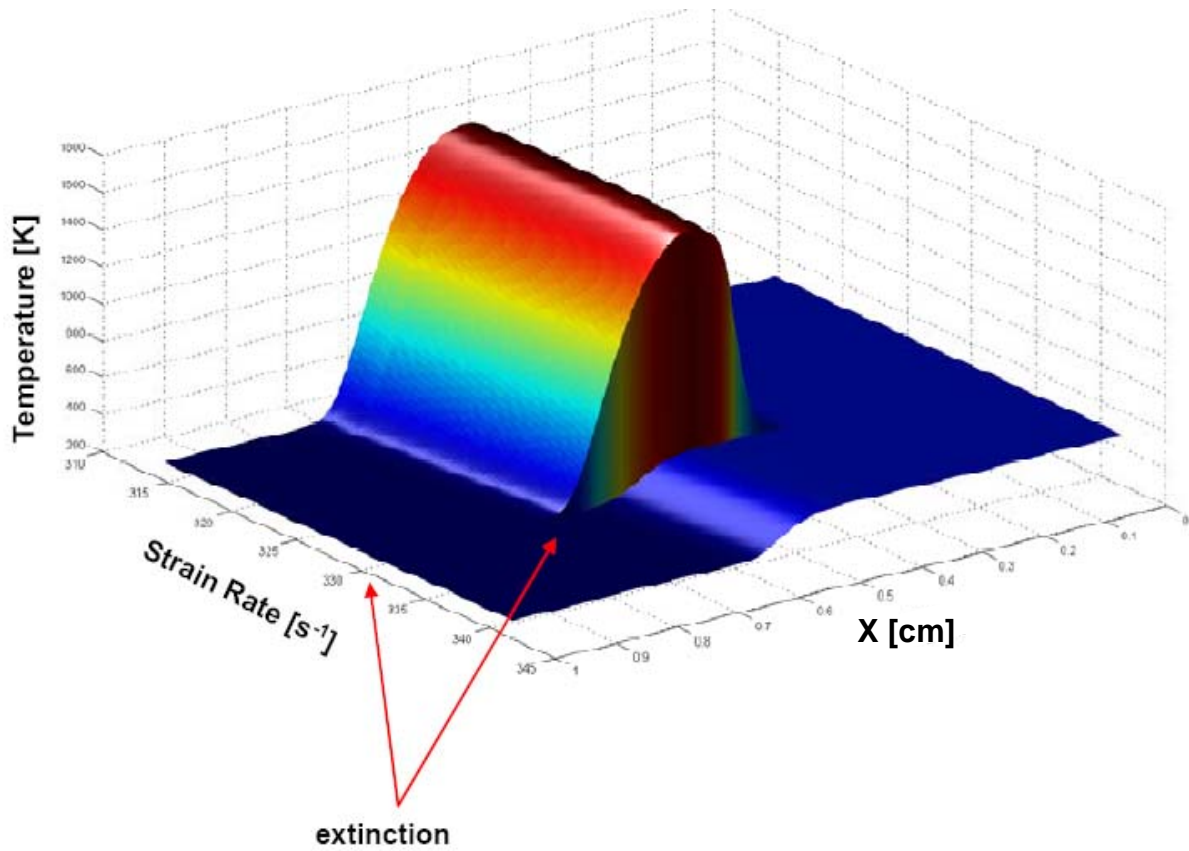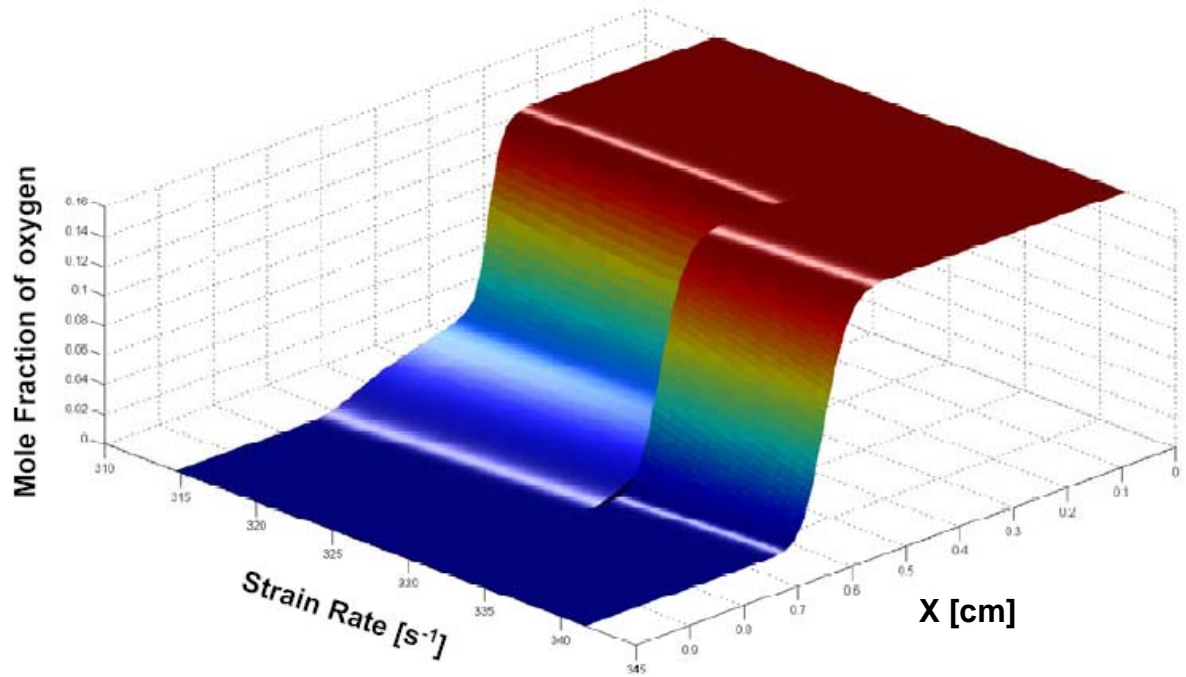

Figure 20 *Fuel strain rate over Flame Temperature and distance between the ducts x at Φ = 0.9 done by Alessio Frassoldati and coworkers at Y_{ox} = 0.18. The fuel mixture temperature T_1 = 483 [K] (210 [°C]) ± 5 [K] and the inert side temperature T_2 = 298 [K] (25 [°C]). The temperature is given in a range of 200 [K] to 1800 [K] in steps of 200 [K]. The strain rate is given in a range of 310 [1/s] to 345 [1/s] in steps of 5 [1/s]. And the distance is given from 0 [cm] to 1 [cm] in steps o f 0.1 [cm].*

Figure 20, done by Alessio Frassoldati and coworkers (Politecnico di Milano, Dipartimento di Chimica) shows the maximum temperature in [K] and the strain rate [1/s] over the distance x between the two ducts where x = 0 [cm] means the exit of duct 1. The high peak of the temperature simulates a flame. Thus, the maximum flame temperature is reached at a distance of 0.5 [cm]. Furthermore, a flame is reached at a strain rate from 314 [1/s] to 335 [1/s]. After strain rate 335 [1/s], the temperature drops to the temperatures of the streams. This means that extinction is reached at 335 [1/s] what is also represented by the extinction arrows in the graph. The maximum temperature of this flame at a Φ = 0.9 is around 1500 [K]. The temperatures at the outlets of duct 1 are T_1 = 483 [K] (210 [°C]) ± 5 [K] and for duct 2 is T_2 = 298 [K] (25 [°C]) which corresponds with the temperatures of the flows.
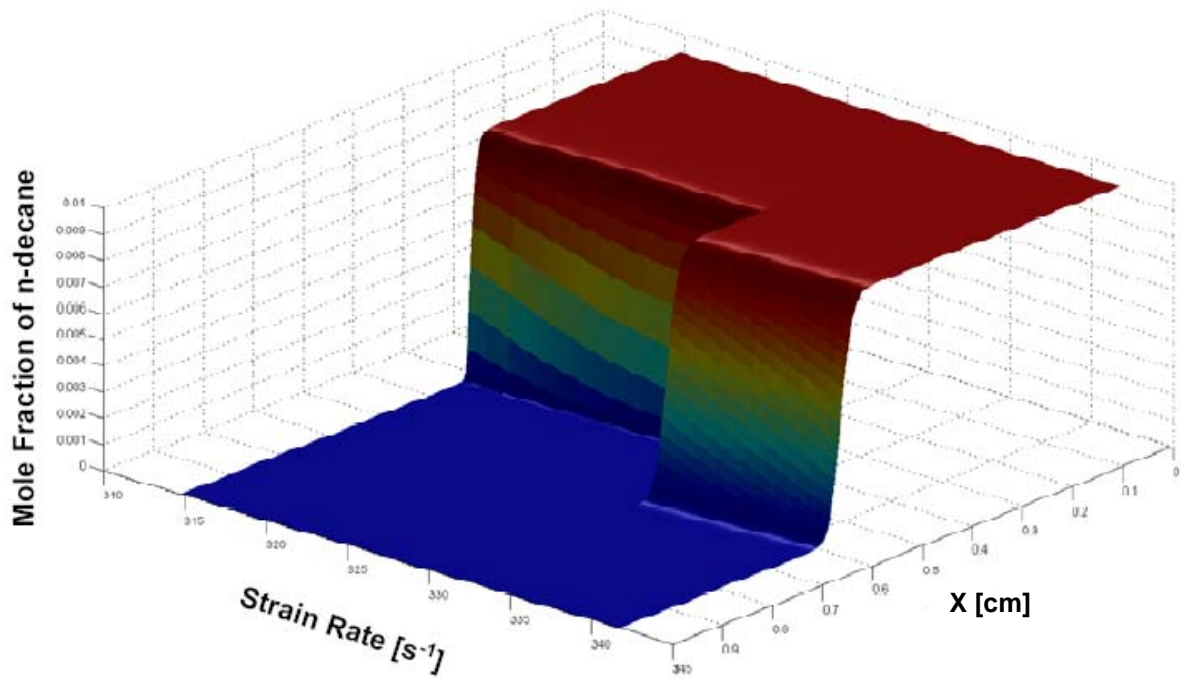
Figure 21 *Fuel strain rate over n-Decane mole fraction and distance between the ducts x at Φ = 0.9 done by Alessio Frassoldati and coworkers at Y_{ox} = 0.18. The fuel mixture temperature T_1 = 483 [K] (210 [°C]) ± 5 [K] and the inert side temperature T_2=298 [K] (25 [°C]). The mole fraction is given in a range of 0 to 0.01 in steps of 0.001. The strain rate is given in a range of 310 [1/s] to 345 [1/s] in steps of 5 [1/s]. And the distance is given from 0 [cm] to 1 [cm] in steps of 0.1 [cm].*

Figure 21 shows the mole fraction of n-Decane over the strain rate [1/s] and the distance between the two ducts x with x = 0 [cm] represent the exit of duct 1 at a Φ = 0.9. At the exit of duct 1 no fuel, in this case n-Decane, has reacted yet, so that in this area the whole mol fraction of n-Decane is still there. This area is the preheat area. When reaching the reaction zone, the fuel starts to get attacked and decomposed. This is when the mole fraction of n-Decane starts dropping to 0 mole fraction (fraction of n- Decane moles of the total number of moles of all components) at an x around 0.4 [cm] in figure 21. Extinction is reached at a strain rate at around 335 [1/s] what means no reaction zone and thus no flame. The n-Decane mole fraction therefore drops as the distance increases.

Figure 22 *Fuel strain rate over Oxygen mole fraction and distance between the ducts x at Φ = 0.9 done by Alessio Frassoldati and coworkers at Y_{ox} = 0.18. The fuel mixture temperature T_1 = 483 [K] (210 [°C]) ± 5 [K] and the inert side temperature T_2 = 298 [K] (25 [°C]). The mole fraction is given in a range of 0 to 0.16 in steps of 0.02. The strain rate is given in a range of 310 [1/s] to 345 [1/s] in steps of 5 [1/s]. And the distance is given from 0 [cm] to 1 [cm] in steps o f 0.1 [cm].*

Figure 22 shows the mole fraction of Oxygen over the strain rate [1/s] and the distance between the two ducts x (x = 0 [cm] means exit at duct 1) at a Φ = 0.9. Extinction is at a strain rate of 335 [1/s] and is noticeable through that step in the distance x. It's the same for oxygen as for n-Decane, when a flame is there, the oxygen mole fraction drops earlier compared to extinction due to the same reasons like already explained for n-Decane. A difference to the n-Decane curve can be seen at lower mole fractions. The oxygen mole fraction doesn't drop that steep at the end compared to n-Decane. At any Φ, there is always more oxygen than fuel, so that some oxygen seems to diffuse through the flame and thus doesn't react or disappear that fast, what can be easily seen in the less steep part of the oxygen mole fraction in the curve in figure 22.

7. Conclusion

The experimental measurements were successfully conducted for all nine fuels (JP-8, Surrogate C, Aachen Surrogate, n-Heptane, n-Decane, n-Dodecane, Methylcyclohexane, 1,2,4-Trimethylbenzene, and o-Xylene). Numerical calculations were successfully done in Chemkin 4.1.1 for n-Heptane using a reduced chemical mechanism by Seiser, H., Pitsch, H., Seshadri, K., Pitz, W.J., and Curran, H. J [24]. The numerical measurements for n-Decane and o-Xylene were realized by Alessio Frassoldati and coworkers (Politecnico di Milano, Dipartimento di Chimica).

The temperatures of the fuel/nitrogen/oxygen mixture T_1 was 483 [K] (210 [°C]) ± 5 [K] for all the experiments and for the pure nitrogen flow, it was T_2 = 298 [K] (25 [°C]).

All the aliphatics show the same extinction behavior and extinguish at a maximum fuel strain rate at around 500 [1/s] for a Φ around 1.15. This agrees with the theory what says that combustion reactions of aliphatic hydrocarbons only vary little to each other because larger hydrocarbons break quicker into smaller more reactive pieces than smaller hydrocarbons. [6, 7, 8, 9]

As already expected from the theory, the aromatics are not very reactive due to their benzene ring structure and therefore extinguish at a lower strain rate (225 [1/s]) than the aliphatics. It's hard to define a peak due to the low strain rates. The maximal fuel strain rate at extinction for o-Xylene is between a Φ of 1 to 1.15 and for 1,2,4-Trimethylbenzene between a Φ of 1.075 to 1.175. Therefore, it was a very challenging task to get good results for the aromatics.

This shows that the extinction varies with the structure of the different components. Structures based on a benzene ring are by far less reactive than aliphatic components. It is very hard to break the benzene ring due to the double bonds compared to the one bond structures of the aliphatics.

The Surrogates extinguish at a Φ of around 1.15 and a maximum fuel strain rate around 375 [1/s]. This is at a fuel strain rate where they are supposed to extinguish, between the fuel strain rates of their aromatic and aliphatic components. This both surrogates also correspond very well with the multi component fuel JP-8 for premixed flames as well as for non-premixed flames as already mentioned before. The surrogates can therefore be used to write chemical mechanisms. [1]

The numerical results for n-Decane done by Alessio Frassoldati and coworkers agree very well with the experimental results for lower Φ values. At higher Φ values, the mechanism predicts slightly higher results (± 100 [1/s]) than the experiments results produces. It is

assumed that those strain rates are too high for the setup because the flame comes too close to duct 1. A relief for this kind of premixed experiments in the future would maybe be to run the experiments with a higher gear (gear 13). Higher strain rates are reached so that V_1 increases and V_2 decreases, what would push the flame further away from duct 1. It is assumed that this would bring the experimental results closer to the numerical results as long as those wouldn't change as well, when changing V_1 and V_2 in the inputs of the program. If this doesn't work, the chemical mechanism must be revised by the Politecnico di Milano, Dipartimento di Chimica. The o-Xylene numerical results agree very well with the experimental results. Numeric and experimental curves have the same progression with a peak strain rate at around $\Phi = 1.15$.

The numerical calculations for n-Heptane using Chemkin 4.1.1 with the chemical mechanism [24] predicts for lower Φ values higher results than the experiments. For higher Φ values numerical and experimental results coincide. The peaks for both results are on different places, the numeric calculation reaches their strain rates peak at around $\Phi = 1.05$ and the experiments at around $\Phi = 1.15$. This assumes that the mechanism [24] has to be improved.

Bibliography

[1] Stefan Humer, Kalyanasundaram Seshadri, Reinhard Seiser, Combustion of jet fuels and its surrogates in laminar no uniform flows, *5th U.S. Combustion Meeting*, 2007.

[2] Tim Edwards and Lourdes Q. Maurice, Surrogate Mixtures to Represent Complex Aviation and Rocket Fuels, *Journal of Propulsion and Power*, 17:461-466, 2001.

[3] J.B. Moss and I.M. Aksit, Modeling soot formation in a laminar diffusion flame burning a surrogate kerosene fuel, *Proceedings of the Combustion Institute*, 31: 3139-3146, 2007.

[4] E. Riemeier, S. Honnet, N. Peters, Flamelet Modeling of Pollutant Formation in a Gas Turbine Combustion Chamber Using Detailed Chemistry for a Kerosene Model Fuel, *Journal Engineering for Gas Turbines and Power*, 126:899-905, 2004.

[5] N. Peters, *Fifteen Lectures on Laminar and turbulent Combustion*, RWTH Aachen, Germany, 1992.

[6] W.C. Gardiner, Jr., *Gas-Phase Combustion Chemistry*, Springer-Verlag New York, Inc, 2000.

[7] J. Warnatz, U. Maas, R.W. Dibble, *Combustion: Physical and Chemical Fundamentals, Modeling and Simulation, Experiments, Pollutant Formation*, Springer Verlag Berlin Heidelberg, 4th edition, 2006

[8] R.M. Fristrom, *Flame Structure and Processes,* Oxford University Press, New York, 1996

[9] Chung K. Law, *Combustion Physics,* Cambridge University Press, New York, 2006

[10] William H.Brown with Christopher S. Foote, *Organic Chemistry, second edition*, Saunders College Publishing, 1997.

[11] Seyhan Ege, *Organic Chemistry: "Structure and Reactivity", 4th edition*, Houghton Mifflin Company, 1999.

[12] Carl L. Yaws, *Chemical Properties Handbook, first edition*, McGraw-Hill Professional, 1998.

[13] Editor: George E.Totten; Section Editors: Steven R. Westbrook and Rajesh J. Shah, *Fuels and Lubricants Handbook: Technology, Properties, Performance, and Testing*, ASTM International, 2003.

[14] Chevron Corporation, *Aviation Fuels Technical Review*, Chevron Corporation, 2004.

[15] L.Q. Maurice, H. Lander, T. Edwards, W.E. Harrison III, Advanced aviation fuels: a look ahead via a historical perspective, *Fuel*, 80:747-756, 2001.

[16] Roger A. Strehlow, *Fundamentals of Combustion*, Robert E. Krieger Company, Inc; Malabar, Florida, 1983.

[17] Edited by Howard D. Ross (chapter 2 by Paul D. Ronney), *Microgravity Combustion, Fire in Free Fall*, Academic Press, San Diego, 2001.

[18] Forman A. Williams, *Combustion Theory: The Fundamental Theory of Chemically Reacting Flow Systems*, The Benjamin/Cummings Publishing Company, Inc., Menlo Park, 1985.

[19] K. Seshadri, The asymptotic structure of a counter flow premixed flame for large activation energies, *International Journal of Engineering Science*, 21:103-111, 1983.

[20] Amable Linan, The asymptotic structure of counter flow diffusion flames for large activation energies, *Acta Astronautica*, 1:1007-1039, 1974.

[21] K. Seshadri and F.A. Williams, Laminar flow between parallel plates with injection of a reactant at high Reynolds numbers, *International Journal of Heat and Mass Transfer*, 21:251-253, 1978.

[22] Reinhard Seiser, *Non-premixed Combustion of Liquid Hydrocarbon Fuels*, Ph. D. thesis Technical University of Graz, Austria, 2000.

[23] K. Seshadri*, Auto ignition and Combustion of Diesel and JP-8, ARO/AFOSR Contractors Meeting in Chemical Propulsion, Boulder, CO*, June 2007.

[24] Seiser, H., Pitsch, H., Seshadri, K., Pitz, W.J., and Curran, H. J., Extinction and Auto ignition of n-Heptane in Counter flow Configuration, *Proceedings of the Combustion Institute*, 28:2029-2037, 2000.

[25] Reaction Design, *Chemkin Theory Manual*, Reaction Design, 2007.

[26] Reaction Design, *Getting Started with Chemkin*, Reaction Design, 2007.

List of Figures

List of Tables

Appendix

Calculation of mass fractions using n-Decane as an example

Calculation of the stoichiometric Fuel/air ratio:

$$\left(Y_{fuel} \middle/ Y_{O_2} \right)_{stoichiometric} = \frac{M_{fuel}}{M_{O_2} \cdot 15.5} = \frac{142.285\,g/mol}{32\,g/mol \cdot 15.5} = 0.287$$

with: $M_{fuel} = M_{n-Decane} = 142.285\,g/mol$ [11, Chemical Properties Handbook, first edition]

$$M_{O_2} = M_{oxygen} = 32\,g/mol$$

Calculation of the oxygen mass fraction Y_{O2}:

$$Y_{N_2} + Y_{O_2} + Y_{fuel} = 1$$

$$\rightarrow \quad \frac{Y_{N_2} + Y_{O_2}}{Y_{O_2}} + \frac{Y_{fuel}}{Y_{O_2}} = \frac{1}{Y_{O_2}}$$

$$\frac{1}{\dfrac{Y_{N_2} + Y_{O_2}}{Y_{O_2}} + \dfrac{Y_{fuel}}{Y_{O_2}}} = Y_{O_2}$$

$$Y_{O_2} = \frac{1}{\dfrac{Y_{N_2} + Y_{O_2}}{Y_{O_2}} + \left(\dfrac{Y_{fuel}}{Y_{O_2}} \right)_{stoichiometric} \cdot \Phi}$$

$$Y_{O_2} = \left(\frac{1}{Y_{ox_{O_2}}} + \left(\frac{Y_{O_2}}{Y_{fuel}} \right)_{stoichiometric} \cdot \Phi \right)^{-1} = \left(\frac{1}{0.18} + 0.287 \cdot 1 \right)^{-1} = 0.1711579$$

Calculation of the fuel mass fraction Y_{fuel}:

$$\left(Y_{fuel} \middle/ Y_{O_2} \right)_{stoichiometric} = 0.287 = \left(Y_{fuel} \middle/ Y_{O_2} \right) \cdot \Phi$$

$$Y_{fuel} = \Phi \cdot Y_{O_2} \cdot 0.287 = 1 \cdot 0.1711579 \cdot 0.287 = 0.0491223$$

Calculation of the nitrogen mass fraction Y_{N2}:

$$Y_{N_2} + Y_{O_2} + Y_{fuel} = 1$$

$$Y_{N_2} = 1 - Y_{O_2} - Y_{fuel} = 1 - 0.1711579 - 0.0491223 = 0.7797197$$

__Average results of Φ and the fuel strain rate at extinction for all fuels__

n-Decane	phi	fuel strain rate [1/s]	n-Heptane	phi	fuel strain rate [1/s]
	0.9	279.25		0.9	262.46
	0.95	355.46		0.95	315.99
	0.975	388.43		0.975	345.39
	1	411.24		1	383.78
	1.025	432.59		1.025	431.66
	1.05	461.00		1.05	464.59
	1.075	477.94		1.075	485.22
	1.1	489.95		1.1	509.51
	1.125	506.64		1.125	517.85
	1.15	513.70		1.15	516.27
	1.175	497.29		1.175	512.56
	1.2	492.53		1.2	508.51
	1.225	486.22		1.225	487.61
n-Dodecane	phi	fuel strain rate [1/s]	Methylcyclohexane	phi	fuel strain rate[1/s]
	0.9	271.74		0.9	263.87
	0.95	339.80		0.95	308.53
	0.975	371.42		0.975	355.71
	1	390.31		1	378.98
	1.025	430.78		1.025	412.32
	1.05	445.55		1.05	425.97
	1.075	482.41		1.075	444.69
	1.1	482.19		1.1	458.34
	1.125	496.78		1.125	474.42
	1.15	496.78		1.15	474.42
	1.175	476.53		1.175	478.56
	1.2	466.42		1.2	458.31
	1.225	457.51		1.225	443.54

JP-8	phi	fuel strain rate [1/s]
	0.9	246.2
	0.925	267.5
	0.95	287.5
	0.975	315.1
	1	330.1
	1.025	365.6
	1.05	381.6
	1.075	386.9
	1.1	391.2
	1.125	395.9
	1.15	398.1
	1.175	386.9
	1.2	374.5
	1.225	359.2

Surrogate C	phi	fuel strain rate [1/s]
	0.95	214.0
	0.975	242.8
	1	269.8
	1.025	294.2
	1.05	328.4
	1.075	341.8
	1.1	362.5
	1.125	372.2
	1.15	374.4
	1.175	377.9
	1.2	376.4
	1.225	368.2

o-Xylene	phi	fuel strain rate [1/s]
	0.975	203.9
	1	222.4
	1.025	228.1
	1.05	228.0
	1.075	228.2
	1.1	226.0
	1.125	223.4
	1.15	219.0
	1.175	211.9
	1.2	209.0
	1.225	200.9

1,2,4-Trimethylbenzene	phi	fuel strain rate [1/s]
	1.025	189.4
	1.05	199.5
	1.075	210.5
	1.125	212.6
	1.15	213.9
	1.175	209.0
	1.2	194.1
	1.225	186.2

Aachen Surrogate	phi	fuel strain rate [1/s]
	0.9	224.3
	0.925	233.2
	0.95	244.0
	0.975	263.1
	1	290.5
	1.025	326.9
	1.05	343.8
	1.075	361.8
	1.1	386.1
	1.125	388.8
	1.15	386.2
	1.175	386.6
	1.2	382.5
	1.225	383.3
	1.25	368.0